FACULTY OF INFORMATION TECHNOLOGY AND ELECTRICAL ENGINEERING
DEGREE PROGRAMME IN WIRELESS COMMUNICATIONS ENGINEERING

MASTER'S THESIS

Control of The Over-The-Air measurements system

Author	Janne Koivuranta
Supervisor	Marko E Leinonen
Second Examiner	Aarno Pärssinen
(Technical Advisor	Sami Korpela)
(Technical Advisor	Kari Saukko)

Month (November) Year (2021)

Koivuranta, J. (2021) Control of The Over-The-Air measurements system. University of Oulu, Faculty of Information Technology and Electrical Engineering, Degree Programme in Wireless Communications Engineering. Master's Thesis, 54 p.

ABSTRACT

Mobile technology is constantly on the move, and it is constantly under development as more efficient and sophisticated telecommunication solutions are needed. As the technology evolves the measurement systems needs to evolve as well. The mobile technology is on the brink of upheaval as we are moving from 4th Generation of wireless communication systems (4G) to 5th Generation of wireless communication systems (5G). The new mobile technology 5G brings new higher frequency bands and new technologies such as massive multiple-input multiple-output and beamforming (BF). In 5G, over-the-air (OTA) measurements are more important because it is virtually impossible to obtain reliable measurement results of BF performance. As the number of antenna elements increases and the antenna spacing decreases, it is very difficult to connect each antenna element to the measuring device with a cable.

In this thesis we made tool to control a whole OTA measurement system. The tool is Python code that is run from the Windows desktop with access to the OTA measurement system. The Python code controls which antennas are taken into measurement, connects those to spectrum analyser, configures spectrum analyser and vector signal analyser and measures the power level for the desired beam set. Once the measurement results are collected, it draws a heatmap that visualizes the performance of the BF.

The measurements were done by using different number of transmitted beams on the same radio unit. Each configuration was measured multiple times to ensure the stability and reliability of the system. The number of transmitted beams in measurement were 2, 4 and 6. From the plotted heatmaps it was concluded that in all measurements all synchronization signal block (SSB) beams were visible and the directions of the SSB beams were as expected. However, in all measurements the power of SSB beam 1 was slightly lower than the other SSB beams which refers to minor issue in beamforming.

As expected, when the number of transmitted beams were 2, the half-power bandwidth (HPBW) was wider and the directivity lower than with 4 or 6 transmitted beams. In measurement results with 2 beams, we had unexpected power drop in the location of antenna 2 in the second SSB beam.

With 4 or 6 transmitted beams we measured approximately same HPBW and directivity. The radiation patterns were also as expected. The performance with 6 beams were better in terms of coverage. With 6 transmitted beams we observed more closely mapped beams which ensures that the user equipment can seamlessly move from beam to another without drop in the signal-to-noise ratio. With 6 beams we also observed slightly wider sector coverage than with 4 transmitted beams.

Key words: over the air measurement, beamforming, synchronization signal block, half-power bandwidth, Python, heatmap

Koivuranta J. (2021) Ilmarajapinta mittausten ohjaus. Oulun yliopisto, tieto- ja sähkötekniikan tiedekunta, elektroniikan ja tietoliikennetekniikan tutkinto-ohjelma. Diplomityö, 54 p.

TIIVISTELMÄ

Mobiiliteknologia on jatkuvasti liikkeellä ja sitä kehitetään jatkuvasti, kun tarvitaan entistä tehokkaampia ja kehittyneempiä tietoliikenneratkaisuja. Tekniikan kehittyessä myös mittausjärjestelmiä on kehitettävä. Mobiiliteknologia on mullistuksen partaalla, kun olemme siirtymässä 4. sukupolven langattomista viestintäjärjestelmistä (4G) 5. sukupolven langattomiin viestintäjärjestelmiin (5G). Uusi mobiiliteknologia 5G tuo uusia korkeampia taajuuskaistoja ja uusia teknologioita, kuten massiivinen moniantennitekniikka ja keilanmuodostus (BF). 5G:ssä ilmarajapinta (OTA) -mittaukset ovat tärkeämpiä, koska pelkästään kaapeleilla on käytännössä mahdotonta saada luotettavia mittaus tuloksia BF-suorituskyvystä. Kun antennielementtien määrä kasvaa ja niiden väliset etäisyydet pienenevät, on hyvin vaikeaa liittää jokainen antennielementti mittauslaitteeseen.

Tässä opinnäytetyössä teimme työkalun koko OTA-mittausjärjestelmän ohjaamiseen. Työkalu on Python-koodi, joka ajetaan Windowsin työpöydältä, jolla on pääsy OTA-mittausjärjestelmään. Python-koodilla ohjataan mitkä antennit otetaan mittaukseen, kytkee ne spektrianalysaattoriin, konfiguroi spektrianalysaattorin ja vektorisignaalianalysaattorin sekä mittaa tehotason halutulle keilaryhmälle. Kun mittaustulokset on kerätty, se piirtää lämpökartan, joka visualisoi BF:n suorituskyvyn.

Mittaukset tehtiin lähettämällä eri määrä keiloja eri mittauksessa samalla radioyksiköllä. Jokainen säteilykuvio mitattiin useita kertoja järjestelmän vakauden ja luotettavuuden varmistamiseksi. Lähetettyjen keilojen lukumäärät olivat kaksi, neljä ja kuusi. Piirretyistä lämpökartoista pääteltiin, että kaikissa mittauksissa kaikki synkronointisignaalilohkon (SSB) keilat olivat näkyvissä ja SSB-keilojen suunnat olivat kuten odotettu. Kuitenkin kaikissa mittauksissa ensimmäisen SSB-keilan teho oli hieman pienempi kuin muiden SSB-keilojen, mikä viittaa lievään vikaan keilanmuodostuksessa.

Kuten odotettiin, kahdella lähetetyllä SSB-keilalla puolen tehon kaistanleveys (HPBW) oli leveämpi ja suuntaavuus pienempi kuin neljällä ja kuudella lähetetyllä SSB-keilalla. Kun lähetettiin vain kaksi SSB-keilaa, havaittiin odottamaton tehon putoaminen toisen antennin kohdalla toisen SSB-keilan mittauksessa.

Neljällä ja kuudella lähetetyillä SSB-keiloilla oli suunnilleen sama HPBW ja suuntaavuus. Molempien tapauksien säteilykuvio oli odotusten mukainen. Kuudella lähetetyllä keilalla suorituskyky oli parempi kattavuuden suhteen. Keilat olivat myös mittauksessa tiiviimmin yhdessä, mikä varmistaa, että käyttäjä voi siirtyä saumattomasti keilasta toiseen ilman signaali-kohinasuhteen putoamista. Kuudella lähetetyllä keilalla myös sektoripeitto oli hieman laajempi kuin neljällä lähetetyllä keilalla.

Avainsanat: ilmarajapinta mittaus, keilanmuodostus, synkronointi signaali lohko, puolen tehon kaistanleveys, Python, lämpökartta

TABLE OF CONTENTS

Contents

FOREWORD

This master's thesis was done to provide a tool to control Over-the-air measurement system and a tool which can be used to verify radio unit's beamforming capabilities.

I express my gratitude to my technical advisors Sami Korpela and Saukko Kari for their support and expertise during the thesis. I want to express my gratitude to Marko Leinonen for instructions and support. I want to also thank Professor Aarno Pärssinen for reviewing the thesis and for the comments.

I want to show my greatest gratitude to my family, girlfriend, and friends. I cannot thank you enough for your support throughout my studies.

Oulu, November 11. 2021

Janne Koivuranta

LIST OF ABBREVIATIONS AND SYMBOLS

3GPP	3rd Generation Partnership Project
5G	Fifth Generation
AF	Array Factor
BF	Beamforming
BTS	Base-station
CRB	Common Resource Block
DAC	Digital-to-Analog Converter
DL	Downlink
DMRS	Demodulation Reference Signal
DSP	Digital Signal Processing
DUT	Device Under Test
DVPA	Dual Polarized Vivaldi Antenna
EPC	Evolved Packet Core
EPS	Evolved Packed System
FDD	Frequency Division Duplex
GSCN	Global Synchronization Channel Number
GSM	Global System for Mobile Communications
HPBW	Half Power Beam Width
IoT	Internet of Things
LOS	Line-of-sight
LTE	Long-Term Evolution
MIB	Master Information Block
MIMO	Multiple Input Multiple Output
NR	New Radio
OFDM	Orthogonal Frequency Division Multiplexing
OFDMA	Orthogonal Frequency Division Multiple Access
OTA	Over-The-Air
PBCH	Physical Broadcast Channel
PCI	Physical Cell ID
PSS	Primary Synchronization signal
QAM	Quadrature Amplitude Modulation
RB	Resource Block
RU	Radio Unit
SA	Spectrum Analyser
SCS	Subcarrier Spacing
SISO	Single Input Single Output
SNR	Signal-to-Noise ratio
SS	Synchronization Signals
SSB	Synchronization Signal Block
SSS	Secondary Synchronization signal
TDD	Time Division Duplex
TDMA	Time-division Multiple Access
UE	User Equipment
UL	Uplink
UMTS	Universal Mobile Telecommunications System

URLLC	Ultra-Reliable Low-Latency Communication
VSA	Vector Signal Analysis
WLAN	Wireless Local Area Network
eNB	LTE base station
gNB	NR base station
mMIMO	Massive Multiple Input Multiple Output

λ	Wavelength
A_e	Effective aperture of antenna
$\mathrm{BW_{RB}}$	Bandwidth of one resource block
c	Speed of light
D	Directivity
D_θ	Directivity for horizontal field component
D_φ	Directivity for vertical field component
E_b	Energy per bit
e_c	Conduction efficiency
e_d	Dielectric efficiency
e_r	Reflection efficiency
e_o	Overall efficiency
f_c	Center frequency
f	Frequency
f_{SSB}	SSB frequency
f_{SSBLow}	Lowest SSB frequency
G	Gain
G_r	Gain of receiver
G_t	Gain of transmitter
kSSB	Offset to SSB in subcarriers
N_0	Noise
N_{RB}	Number of resource blocks
P_r	Received power
P_t	Transmitted power
P_{rad}	Total radiated power
RBOffset	Offset to SSB in resource blocks
R	Distance between receive and transmit antenna
U	Radiation intensity
U_0	Radiation intensity of isotropic source

1 INTRODUCT

Over-The-Air (OTA) testing plays a major role in the research and development of New Radio (NR) technology. The importance of OTA measurements for product development is greater than that of the previous mobile networks with WCDMA (3G) or LTE (4G). This is because 5G technology needs to utilize the beamforming (BF) to the improve the coverage of the cells as the 5G is used in higher frequency bands. The BF brings its own new challenges for locating and tracking the user equipment (UE) and performing measurements and reporting.

In this thesis I implemented a Python code which is used to control the whole OTA measurement system. It will control everything from the antennas all the way to the spectrum analyser. However, the main purpose of the code is to plot heatmaps for each beam individually. From the heatmap we can see if the directions of the beams are as expected and if the powers are in expected level. The code is used to verify every radio unit (RU) before it is used it other testing.

The thesis will firstly go through the basics of the LTE and NR. Then we will discuss about the synchronization signal block (SSB) and its most crucial characteristics. After that we will understand the basics of multiple-input multiple-output (MIMO), massive MIMO (mMIMO) and beamforming techniques. On the third chapter we will go through the device under testing and it's parameters like antenna arrays, beamwidths, directivity, gain and beam sets. On the fourth chapter we will study the test environment itself and the tools which are used and controlled in the measurements. After that we will go through step-by-step the Python code and we will explain the functions and most important parameters of the code. Finally, we will execute measurements with three different beam sets for the same RU and analyse the results. On the last section is the summary and conclusions of the thesis work

2 CURRENT TELECOMMUNICATION SYSTEMS AND THEIR EVOLUTION

2.1 Long-Term Evolution

Long-term evolution (LTE) mobile technology was introduced by 3rd Generation Partnership Project (3GPP) in release 8 in December 2008. The motivation for developing LTE was the demand for higher data rates, Packet Switch optimised system and high spectral efficiency. The LTE uses new access network, Evolved Packet System (EPS), to optimise the system to use Packet Switching. Unlike previous mobile technologies, like the Global System for Mobile Communications (GSM) and Universal Mobile Telecommunications System (UMTS), the LTE uses Evolved Packet Core (EPC) which is completely based on IP protocol.

In LTE, higher data rates are achieved with orthogonal allocation strategies, bandwidths up to 20 MHz, Quadrature Amplitude Modulation (QAM) order up to 64 and with spatial multiplexing technique which utilizes up to four layers in downlink (DL) direction. The orthogonal allocation strategies are Orthogonal Frequency Division Multiple Access (OFDMA) with Frequency Division Duplexing (FDD) systems and Time Division Multiple Access (TDMA) with Time Division Duplexing (TDD) systems. In the uplink (UL) direction the theoretical peak data rate is 75 Mbits/s and in the DL direction the theoretical peak data rate is 300 Mbits/s. [1]For the reference the highest theoretical data rates in DL for UMTS, which uses Code Division Multiple Access (CDMA), is 2 Mbits/s. [2]Also the average spectral efficiency with LTE which utilizes OFDMA is 1.5 bits/s/Hz/cell as in UMTS it's only 0.24 bits/s/Hz/cell. The average spectral efficiency describes how much data can be transmitted in a second per Hz per cell in use. [3]

The OFDMA is a multiple access technique where the used bandwidth is divided in frequency dimension and in time dimension to multiple subcarriers. The different subcarriers are orthogonal to each other to mitigate the interference between subcarriers and partially overlapping each other to ensure the efficient utilization of the spectrum. Subcarrier's bandwidth is much smaller than the coherence bandwidth of the channel as we aim to have flat fading channel. In flat fading channel the fading is independent from frequency and all subcarriers experience approximately same fading. When we transmit user data, it is transmitted parallel via each subcarrier. In OFDMA the different subcarriers can be shared dynamically between different users so it can server multiple users at the same time. It is said, that OFDMA combines frequency division multiple access (FDMA) and time division multiple access (TDMA).[4] In Fig. 1 it is illustrated how different subcarriers are allocated in OFDMA over frequency and time.

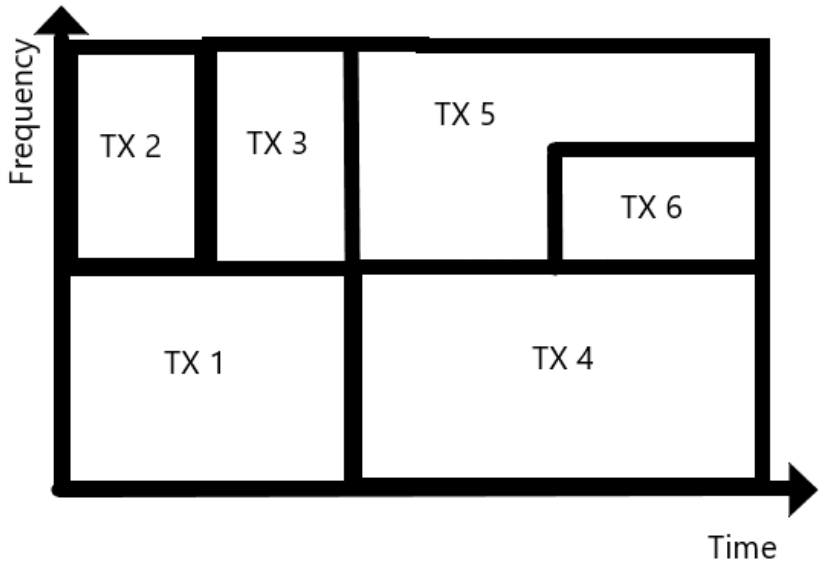

Figure 1. Subcarriers allocation of multiple users in OFDM manner, where TX# represents allocation of each user

The OFDM transmission scheme is used in LTE in FDD and TDD modes in base-stations (BTS). In FDD the used bandwidth is shared between symmetric segments of UL and DL transmission channels. Different radio channels are also separated with sufficient amount of guard band to prevent interference among different channels. From this we can conclude that to have 9 MHz bandwidth for DL transmission and 9 MHz bandwidth for UL transmission it is required to have 20 MHz of bandwidth as it is required to have 1 MHz guard band for each side of the channel. With channel bandwidth of 5 MHz we need guard band of 250 kHz on each side of the channel which leaves us with channel bandwidth of 4,50 MHz which is again symmetrically shared between DL and UL channels. [5]This is not good from spectral efficient point-of-view. Also, as the guard period is not useable for any transmission it is wasting spectrum. The advantage of having two separate channels for DL and UL transmissions is to have simultaneous reception and transmission which decreases latency of the system. [6]

In TDD the UL and DL channels shares the same bandwidth, but in different time slots. This significantly increases the spectral efficiency, but on the other hand increases latency as DL and UL transmissions cannot be done simultaneously. Also, as there must be guard periods between different time slots, some part of the spectrum must be sacrificed. One advantage of TDD is asymmetric traffic model. In TDD it is possible to change the DL/UL slot ratio to optimize the traffic model for the capacity requirements. It is possible to share the DL/UL slots equally to get equal capacity as in FDD, but it is also possible to share more slots for DL and less slots to UL. In most cases it is required to have more DL capacity than UL capacity and with optimized slot allocation higher spectral efficiency is achieved. [7]

In TDD the used transmission scheme TDMA. In TDMA the different subcarrier transmissions are separated in time domain. On other words each subcarrier has its' own time slot within the time frame. For example, we can have frame which time duration is 10 milliseconds, and we have 20 time slots within that frame. This means that each subcarrier occupies the whole bandwidth for itself

for the time slot which in this example lasts 0.5 milliseconds. Different slots can be DL slots or UL slots and can be allocated to different users. There are multiple different possible frame structures and as it is mentioned above, the allocation of DL and UL slots can be optimized for different use cases. [8]However, between TDD and FDD technologies the FDD is more widely used in LTE because of the existing spectrum assignments and earlier mobile technologies. [9]In Fig. 2 is illustrated how different subcarriers are allocated in frame.

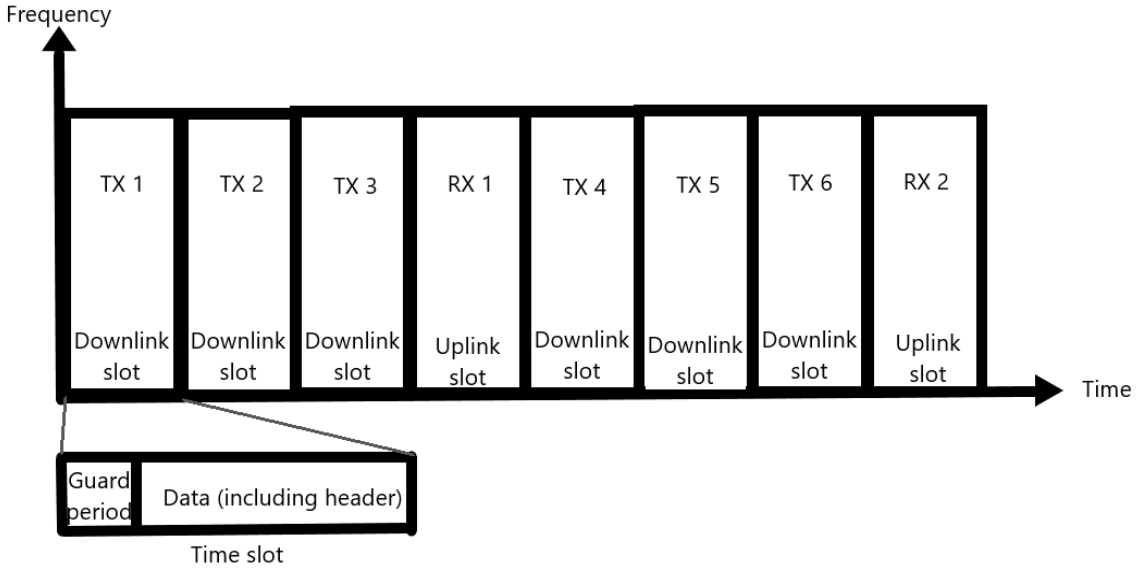

Figure 2. TDMA with ¼ UL/DL slot allocation "xX#", where x refers UL or DL direction and # associated user.

2.2 New Radio

Like every past mobile technology, the NR also aims for more efficient telecommunication solutions to improve the system capacity, cell coverage and data rates to answer the continuously increasing demand from users. But the need for NR, also known as fifth generation (5G) mobile technology, is more than that. It enables new use cases which requires also very low latency and very high reliability. For example, Internet of Things (IoT) requires having an extreme coverage, capacity to handle very large number of devices with very low device cost and energy consumptions. Another use case example is ultra-reliable low-latency communication (URLLC) which enables very low latency data communication between devices with high reliability. [10]However, unlike previous mobile technologies, the NR is focusing more on improving the spectrum utilization rather than spectrum efficiency. The spectrum utilization is measured in how many bits can be included per Hertz per unit area (bits/Hz/Unit area), where the unit area can mean for example cell or site, as the spectrum efficiency is measured in how many bits can be included in Hertz (bits/Hz). [11]In LTE the occupancy rate of the allocated bandwidth is 90% and in NR it can be as high as 98%. This has direct impact on the performance of the communication system as we have less waste. The reason why spectrum utilisation is more important is that improvements in spectral efficiency are constrained by noise and improving

modulation and coding schemes are inefficient as we have almost reached the theoretical channel capacity with LTE. [12]This theoretical channel capacity limit is also called as Shannon limit. [11]

The Shannon limit defines the lowest Signal-to-Noise ratio (SNR) which is needed for reliably data transmission. [12]This limit is calculated with equation (1)

$$\frac{E_b}{N_0} = \frac{1}{log_2 e} = -1.6\ dB, \tag{1}$$

where E_b is energy per bit and N_0 is the noise.

One of the key features of 5G is the wider range of spectrum as 5G supports frequency bands from below 1 GHz up to 52.6 GHz where the maximum channel bandwidth can be 400 MHz. Also, with carrier aggregation it is possible to combine for example three 400MHz cells which produces "super cell" with bandwidth of 1200MHz. NR is also capable to utilize unlicensed spectrum. [13]In comparison, LTE FDD supports spectrum from 700 MHz to 2600 MHz and with LTE TDD up to 5900 MHz with 20MHz of channel bandwidth. The frequency bands for LTE are visible in Appendix 1.[13] In Release 15 the 3GPP introduced that the allocated spectrum for 5G is divided to two regions: Frequency Region 1 (FR1) and Frequency Region 2 (FR2). The FR1 contains frequency bands which are lower than 6GHz with maximum bandwidth of 200 MHz and the FR2 contains frequency bands from 24.25 GHz to 52.6 GHz with maximum bandwidth of 400 MHz. [10][14]The FR1 frequency bands are visible in Appendix 2 and the FR2 frequency bands are visible in Appendix 3.

2.3 Synchronization Signal Block

Synchronization Signal Block (SSB) is essential to have connection established between UE and LTE BTS (eNB) or NR BTS (gNB). UE also uses information contained from SSB to trigger handovers and to perform beam management. SSB contains basic system information of gNB/eNB and crucial information, such as physical cell ID (PCI), for identifying the cell. If multiple SSB is transmitted the SSB contains also it's index. SSB is built from Synchronization Signals (SS) and physical broadcast channel (PBCH) where the first part is used for cell search procedure and latter for acquiring basic system information. In cell search procedure UE acquires time and frequency synchronization and detects the PCI of the cell. The SS consists of two parts: The Primary Synchronization signal (PSS) and the Secondary Synchronization signal (SSS). The PBCH contains Master Information Block (MIB) and Demodulation Reference Signals (DMRS) where the latter is used to successfully decode the MIB. The MIB contains basic system information. In the time domain the length of the SSB is four Orthogonal Frequency Division Multiplexing (OFDM) symbols [15][16]The structure for SSB is illustrated in Fig. 3.

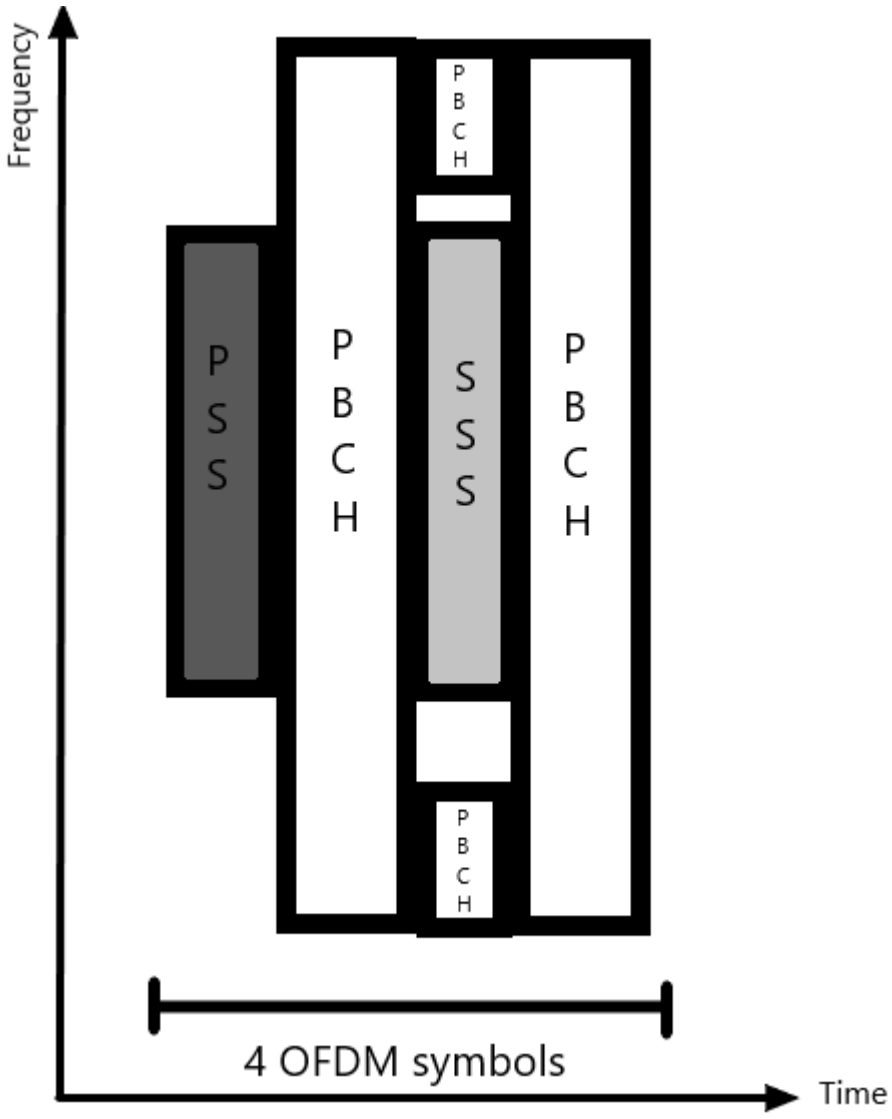

Figure 3. SSB structure where in horizontal axis is time and in vertical axis is frequency.

The size of the SSB in frequency domain is 20 resource blocks (RB). One RB consists of 12 subcarriers which equals to total amount of 240 subcarriers. [17]The total amount of available RBs depends on the Sub Carrier Spacing (SCS) and on the bandwidth in use. In table 1 and table 2 is visible the total number of RBs with different SCS and bandwidths for FR1 and FR2. [18]

Table 1. Number of resource blocks (N_{RB}) of SCS for FR1 [18]

	BW (MHz)										
SCS (kHz)	5	10	15	20	25	30	40	50	60	80	100
	N_{RB}	N_{RB}	N_{RB}	N_{RB}	N_{RB}	N_{RB}	N_{RB}	N_{RB}	N_{RB}	N_{RB}	N_{RB}
15	25	52	79	106	133	160	216	270	N/A	N/A	N/A
30	11	24	38	51	65	78	106	133	162	217	273
60	N/A	11	18	24	31	38	51	65	79	107	135

Table 2. Number of resource blocks (N_{RB}) of SCS for FR2 [18]

	BW (MHz)			
SCS (kHz)	50	100	200	400
	N_{RB}	N_{RB}	N_{RB}	N_{RB}
60	66	132	264	N/A
120	32	66	132	264

From tables 1 and 2 it is visible that the larger is the SCS the smaller amount of RBs can fit in the bandwidth. This is due to fact that when the SCS increases the subcarriers within the RB needs more resources in frequency domain. With the SCS of 15 kHz one RB occupies 180 kHz of bandwidth and with the SCS of 30 kHz one RB occupies 360 kHz of bandwidth. It is important to understand that SSB and other resources can use different SCS value. For example, if common SCS is 30kHz and the bandwidth of the channel is 5 MHz the total number of available RBs measured with SCS of 30kHz is only 11. In this case the SSB needs to be configured with the SCS of 15 kHz so that it's 20 RBs can fit in the channel. [19]

As the SSB needs only 20 RBs and the available number of RBs can be even 273 the transmission of the SSB does not occupy the whole bandwidth. In fact, the SSB can be transmitted in different parts of the bandwidth. The location of the SSB in the frequency domain is defined by the Global Synchronization Channel Number (GSCN).[18] More precisely, the GSCN defines the position of the first subcarrier of the 10^{th} RB of the SSB e.g., the center frequency of the SSB.

In our thesis work it is crucial for spectrum analyser to know the exact location of the SSB in frequency. This information is provided with two parameters: Offset-To-Point-A and k-SSB. These parameters are illustrated in Fig. 4 below.

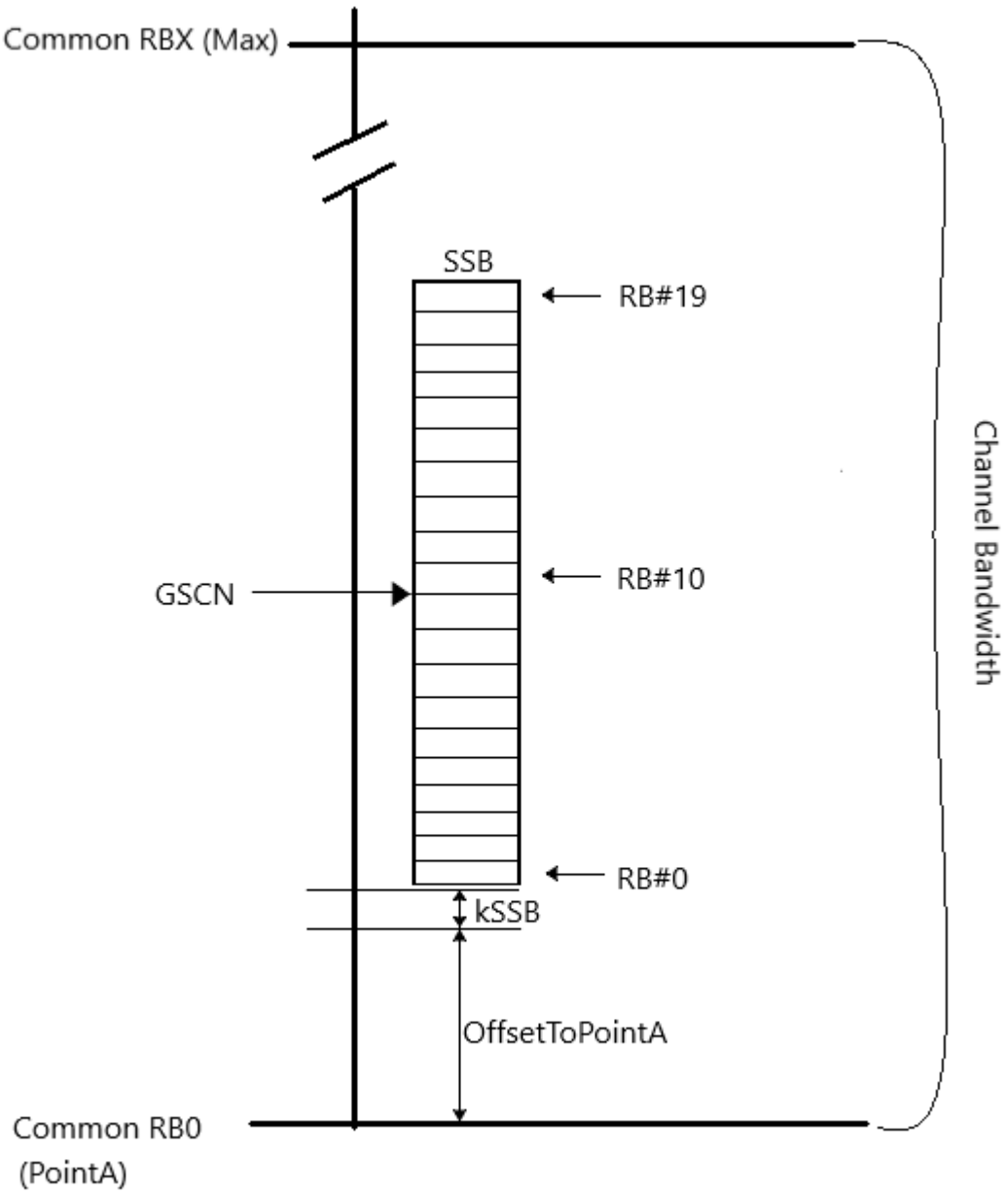

Figure 4. The location of the SSB in the channel bandwidth

The Point A represents the first subcarrier of the lowest resource block of the carrier bandwidth. The resource blocks which are numbered from the lowest part of the carrier to the highest part of the carrier are also called as Common Resource Blocks (CRB). Offset-To-Point-A is the offset between the Point A and the first subcarrier of the SSB and it is measured in RBs. The k-SSB is the subcarrier offset between the last offset RB of Offset-To-Point-A to the first subcarrier of the SSB. These values can be zero if the first RB of the SSB starts immediately after CRB. It is important to note that the values of Offset-To-Point-A and k-SSB are always measured and reported with SCS of 15 kHz in FR1 and with SCS of 60 kHz in FR2. In case where multiple SSBs are transmitted the different SSBs utilizes same frequency resources and thus the values Offset-To-Point-A and k-SSB are identical

with every transmitted SSBs.[18] The separation of these SSBs occurs in time domain as it is visible in Fig. 5.

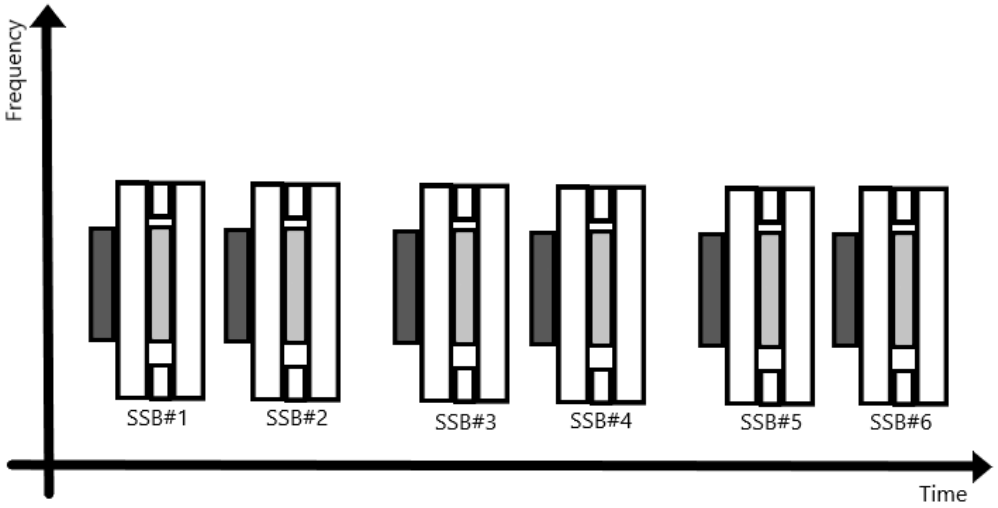

Figure 5. Multiple SSB transmission case with six SSBs.

Regarding to which frequency and SCS is used, the transmission of SSB may have different types. In table 3 is introduced different SSB cases.

Table 3. SSB cases from A to E [17]

Case	Frequency band	SCS
A	FR1	15 kHz
B	FR1	30 kHz
C	FR1	30 kHz
D	FR2	120 kHz
E	FR2	240 kHz

As we compare case B and case C in table 3, we can see that they are identical in the frequency domain. However, in time domain there is difference. In case where multiple SSBs are transmitted, two SSBs forms a pair and with case B the SSBs which forms a pair are mapped more closely to each other than in case C. In Fig. 5 there is visible transmission of six SSBs with case C. If SSBs within SSB pair, for example the first pair (SSB#1 and SSB#2), would be attached to each other without no time delay between, the transmission would be case B.

Regardless the case of the SSB transmission, the SSBs are always transmitted within the first half of the frame. With FR1, in multiple SSB transmission case, SSBs are transmitted every 20ms e.g., every other frame. In case where we transmit only one SSB the SSB can be sent within every frame. [17]In comparison in LTE there is only one pattern for transmitting SSBs. Also, in LTE SSB the SS and PBCH are allocated equal number of subcarriers as in NR SSB SS requires less resources in frequency domain which leaves more resources for other transmissions. As it is

visible in Fig. 3 part of the PBCH is transmitted in the same time slots as SSS. This makes NR more flexible than LTE.

In NR we use technique beamforming which is explained in detail in chapter 2.5. When we transmit multiple SSBs the each SSB is transmitted in its own beam which radiates to certain direction in the sector. This technique is called beam sweeping and by utilizing it it's possible to cover the whole sector. This is crucial because multiple UEs can be lying all around the gNB or even moving. UE measures the strength of the each SSB and because different SSBs has their unique SSB index the UE identifies the SSB which has the strongest signal strength and uses it to trigger attach procedure. For example, UE1 can be on the other side of the sector and UE2 on the other side. In this case the UE1 may hear the SSB with index zero strongest and uses that beam to trigger the attach procedure. On the same time UE2 may hear for example SSB with index five strongest and triggers attach procedure for that beam. The number of transmitted SSB beams is determined how many SSBs are configured to be transmitted from gNB. [17]

2.4 MIMO

Multiple Input Multiple Output (MIMO) is technique used in telecommunications where signal is transmitted and received with multiple antennas. With MIMO it is possible to increase coverage or capacity of the radio communication channel depending on the used MIMO transmission strategy. There are two different transmission strategies: spatial diversity and spatial multiplexing.

The idea of using spatial diversity is to obtain diversity gain and improve reliability and coverage of the communication channel. In spatial diversity the same information is transmitted to the UE from multiple transmit antennas to multiple receiving antennas. The transmit and receive antennas are located sufficiently far apart of each other so that signals transmitted from different antennas experiences independent fading and hence the probability that one of the signal paths is strong enough is increased. In receiver the different signals received by different antennas are coherently combined to increase the Signal-to-Interference-and-Noise-ratio (SINR). Spatial diversity technique is an optimal transmission strategy in low SINR region where the coverage and reliability are the main concern. [20][21]In Fig. 6 is illustrated how spatial diversity technique is utilized with three transmit antennas.

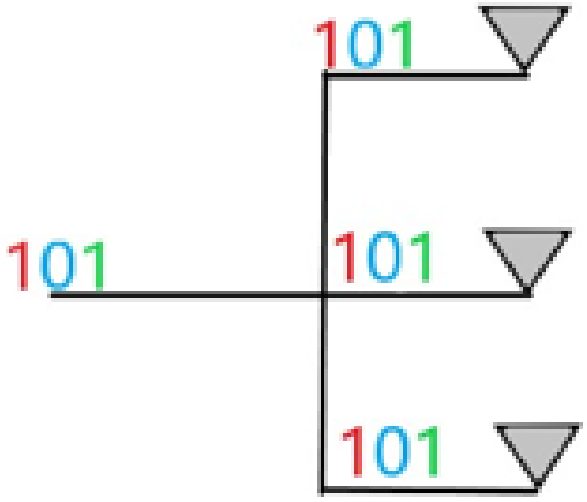

Figure 6. The spatial diversity technique where same information is shared to three transmit antennas.

With the spatial multiplexing technique, the information is split to the different transmit antennas and each data stream is received by different receive antenna. Receiver then combines the received different data streams to one data. For example, with 4-by-4 MIMO we can have four independent data streams which are combined in receiver. 4-by-4 MIMO channel is also known as channel which has 4 layers or channel which rank is 4. With this example we can achieve four times higher data rate than with Single Input Single Output (SISO) method which rank is one. [21]In Fig. 7 is illustrated how spatial multiplexing technique is utilized with multiple transmit antennas.

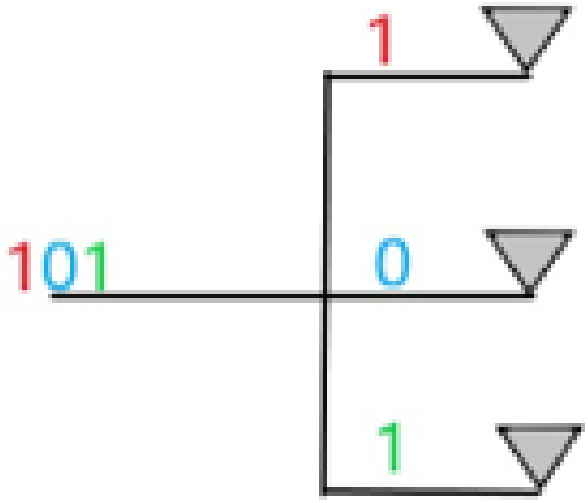

Figure 7. The spatial diversity technique where the three transmit antennas has its own independent data.

2.5 Massive MIMO & Beamforming

With NR and utilization of higher frequency bands the main concern is the coverage and reliability of the communication channel. To improve these factors the NR brings two new technologies with it. These are massive MIMO (mMIMO) and beamforming (BF).

Very often BF and mMIMO are spoken as they are the same thing. However, this is not quite the case. BF is more like how antenna elements works together and mMIMO defines the amount of antenna elements in radio. The rough definition for mMIMO is that system has more antenna elements than UEs. In NR, generally radios with 32 to 64 antenna elements are classified as mMIMO radios. Utilizing mMIMO improves spectral efficiency, communication reliability and link capacity. [22][23]

In BF the same data is transmitted from multiple antenna elements towards the UE. To utilize the spatial multiplexing vertical and horizontal polarities can contain independent data. The phase and magnitude of these antenna elements are adjusted to create desired radiation pattern to the desired direction. This radiation pattern is called as a beam. The magnitude adjustments should be done in a way that the antenna elements' radiation patterns combine constructively in the desired direction and destructively to anywhere else. This way we can have maximum power in the direction of the main lobe and minimum power to the side lobes. Side lobes are produced every time BF is utilized and causes interference to other beams, but with correct tapering strategy side lobes can be reduced to the minimum. With phase adjustments we can tilt and steer the beam to the desired direction. Tilting the beam means adjusting the beam direction vertically and steering the beam means adjusting the beam horizontally. The usage of BF improves capacity, coverage and reliability of the system [22][24]

In NR the BF and mMIMO technologies are working together. In MIMO each antenna element works individually, but in mMIMO we can use all of the antenna elements together to form one large antenna array which is used to form one wide beam. The other option is to divide antenna elements to multiple smaller antenna arrays to form multiple narrow beams which are transmitted to the UEs. As we go higher in frequency bands the size of antenna elements goes smaller which means we can pack more antenna elements to smaller area and thus we can transmit higher number of beams to the air interface. Also, the usage of higher number of transmitting antenna elements enables large-scale spatial multiplexing, higher directivity, and lower amount of energy leakage between UEs. [22][24][25]There are three different architectures for BF: digital BF, analog BF and hybrid BF. In the Fig. 8 is shown beamforming case where all of radio's the antenna elements are used to form one beam.

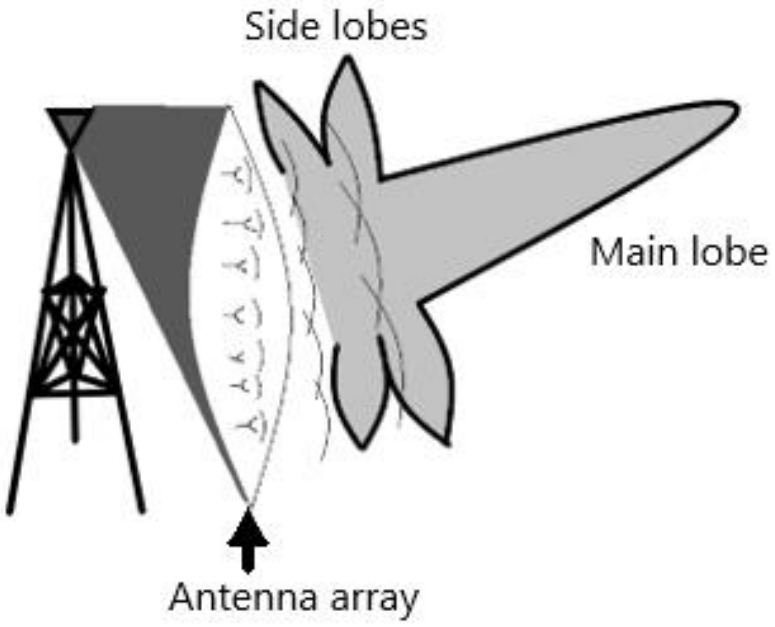

Figure 8. Beamforming illustration

2.5.1 Digital beamforming

In digital beamforming architecture every antenna element has its own baseband port and analog RF front-end. With digital implementation Digital Signal Processing (DSP) has the responsibility of adjusting phase and magnitudes of the signal. Digital BF enables frequency selective beam directions and continuously adjustable beamforming weights. [26]Overall digital BF has better flexibility, but has higher cost, power consumption and complexity than other beamforming architectures. This is because every antenna element has its own RF chain. As we can see from Fig. 9, within each RF chain there is a Digital-to-Analog Converter (DAC) and BF weight. DACs has naturally high-power consumption and costs, but with higher frequencies it is even higher. The digital BF architecture is mainly used with FR1 bands where the number of antenna elements are less, and power consumption of multiple DACs are less than with FR2 bands.[27]

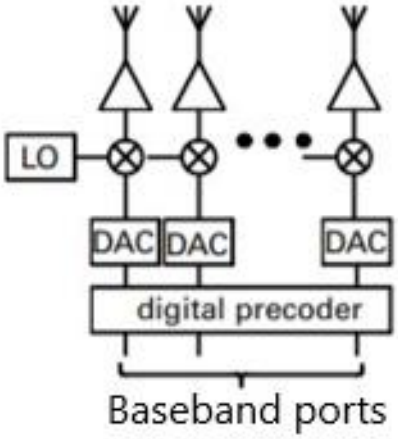

Figure 9. Digital beamforming architecture

2.5.2 Analog beamforming

Digital beamforming architecture is not conventional to use with FR2. This is because with higher frequencies it's possible to pack higher amount of antenna elements in the radio and with digital beamforming architecture every antenna element requires its own RF chain. This implementation has high cost and power consumption. Its more conventional to use other method with FR2 radios and it's called analog beamforming. As it is visible in Fig. 10, analog beamformer has only one baseband port which feeds the signal to the DAC. After that the signal is converted to analog, the antenna weights are added to the signal, and it is fed to every antenna element in that antenna array.

In analog beamformer, phase shifters are used to adjust the phase of the signal. Analog phase shifters imposes a constant modulus constraint on the elements of the beamformer and thus analog beamformer has more poor performance than digital beamformer. With analog BF it is not possible to create complicated radiation patterns such as creating nulls to desired directions which causes inter-beam interference. However, analog BF has low power consumption and low complexity and is thus preferred in FR2 bands more than digital BF. [26][27]

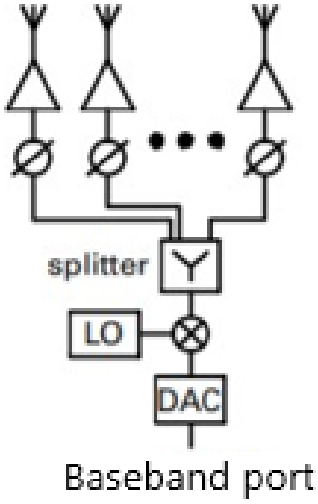

Figure 10. Analog beamforming architecture

2.5.3 Hybrid beamforming

Hybrid beamforming is a solution where analog beamformer and digital beamformer are combined. It is a compromise between flexibility and complexity to the advantages from both architectures. Hybrid BF has smaller amount of baseband ports than digital implementation, but more than in analog implementation. The baseband ports are connected to digital precoder as in digital BF, but after that the architecture follows analog BF architecture. Like we can see in Fig. 11, it can be said that there are multiple smaller analog BF networks connected to the digital precoder.

Hybrid beamformer is great alternative to be used in FR2 RUs because with hybrid BF we can create more complicated radiation pattern and unlike in analog implementation we can create nulls for the desired direction and minimize the inter-beam interference. With hybrid BF we can also achieve higher flexibility and performance than in analog BF, but with less cost and power requirements than in digital BF.[27] Hybrid BF provides also higher gain than analog implementation because of the digital/hybrid signal processing methods. Hybrid beamforming is widely used in both frequency ranges. [28]

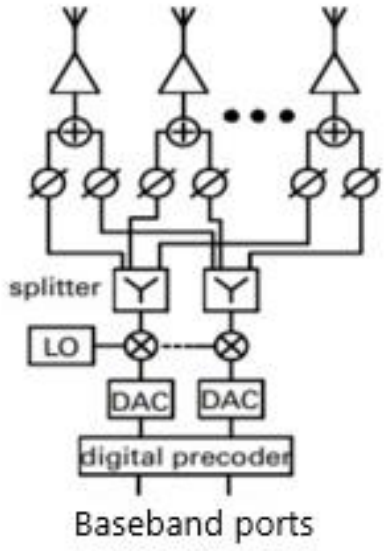

Figure 11. Hybrid beamforming architecture

3 DEVICE UNDER TEST

Device Under Test (DUT) is a product which is undergoing testing. [29]In this thesis work we refer DUT as a RU. During this chapter we are going through the most important factors of DUT.

3.1 Antennas and antenna arrays

The higher frequency is used the lower is the wavelength. This can be seen from equation

$$\lambda = c/f, \tag{2}$$

where λ is the wavelength of the used frequency f and c is the light of speed which is $2.99 * 10^8$ m/s. Frequencies with short wavelength has lower coverage than frequencies with longer wavelength as short wavelengths have high propagation and penetration losses. On the other hand, high frequencies enable higher data rates due to available spectrum bandwidth and enables usage of bigger user groups as the channel bandwidth increases. As it is mentioned earlier FR1 maximum bandwidth is 200 MHz as in FR2 it is even 400 MHz.

Other advantage of utilizing higher frequencies is that with short wavelengths the physical size of antenna elements is smaller and the antenna spacing is shorter. In mmW antennas the most often used antenna spacing is half wavelength because it enables low side lobe levels with beam steering. [30]This means that we can pack more antenna elements in the same area which increases the electrical size of the antenna and this directly means higher gain. [12]It can be mathematically proven with equations below. As 3 dB is equal to doubling the power, the gain G is

$$\mathrm{G} = 2 = 3dB, \tag{3}$$

which means 6 dB equals to four-time power

$$\mathrm{G} = 2 * 2 \triangleq 3dB + 3dB = 6dB. \tag{4}$$

From equation 4 we can approximate that if the gain of one antenna element is three it equals to 5 dBi, where dBi defines the gain of an antenna compared to hypothetical isotropic antenna. If we have four antenna elements the gain is G = 5 dBi + 6dB = 11 dBi.

With the SA and VSA used in this thesis the SSBs will be measured in dBV. The dBV is decibel unit specially for measuring voltage and thus the decibel is relative to voltage i.e., dBV = 0 = 1.0V. [31]In 50 Ohm system, like our SA, dBV can be converted to dBm as

$$Value\ in\ dBm = Value\ in\ dBV + 13dB, \tag{5}$$

where dBm is decibel relative to milliwatts. [32]. From equation 5 we can calculate that -40 dBV equals to -27 dBm.

From receiving antenna perspective higher amount of antenna elements leads to larger effective aperture of an antenna $A_{e,}$

$$A_e = \frac{\lambda^2}{4\pi} G, \tag{6}$$

as the gain is higher. Effective aperture of an antenna describes how effective an antenna is receiving signal. The higher the effective aperture of the receiving antenna is the higher is the receiving power P_r

$$P_r = \frac{P_t}{4\pi R^2} G_t A_e, \tag{7}$$

where G_t is the gain of transmit antenna, P_t is the power of the transmit antenna and R is the distance between transmit and receive antenna. The equation 7 can be also written as

$$P_r = \frac{P_t G_t G_r \lambda^2}{(4\pi R)^2}, \tag{8}$$

where G_r is the gain of receive antenna. This equation 8 is known as Friis Transmission Formula which is one of the most fundamental formulas in antenna theory. If we substitute equation 2 to equation 8, we can see that the received power decreases with higher frequencies which means that the coverage is indeed lower with short wavelengths. [33]This phenomenon occurs because the antenna size shrinks with decreasing wavelength. However, if we keep the antenna size constant, the gains of antennas increase as the wavelength decreases and thus results to improved received signal strength in ideal line-of-sight (LOS) condition. [34]

A group of antenna elements is called as an antenna array. Antenna elements within one group are typically thought as identical. In RU there can be multiple smaller antenna arrays or one large antenna array. Antenna arrays are used when radiation requirements, like requirement for BF, cannot be implemented with traditional single antenna element. With identical antenna elements in antenna array there is at least six variables which can be adjusted to shape the array's radiation pattern. These are: relative patterns, relative position, excitation amplitude and excitation phase of single antenna elements, geometrical configuration. How accurately the coupling is done has also an effect on the radiation pattern. [22]

3.2 Radiation pattern

The radiation pattern describes the radiation properties of the radiating antenna or antenna array. It can be defined with graphical representation or with mathematical function. Radiation pattern can be defined as 3D or 2D function. To capture 3D radiation pattern multiple 2D radiation patterns, or pattern cuts, must be taken with fixed azimuth or elevation angle and by varying the other. Radiation pattern consists of main lobes, side lobes and back lobes. The radiation patterns can define different properties, like gain, directivity and electric field. [35]

If antenna's receiving and transmitting radiation patterns are identical, the antenna fulfils the reciprocity theorem. Reciprocity theorem concludes that the transmit and receiving properties of an antenna or antenna array are identical. This means that if we know the radiation pattern of transmitting antenna, you also know the radiation pattern if the antenna is in receiving mode. The reciprocity of the DUT should be always considered. First the hardware should be checked if it fulfils the reciprocity theorem's requirements. For example, FDD systems does not fulfil reciprocity theorem since the DL and UL channels are separated more than a coherence frequency bandwidth. But TDD systems holds channel reciprocity if the DL and UL transmissions are within the channel coherence time. [36]Coherence frequency bandwidth and coherence time defines the window size where the channel stays constant in terms of bandwidth or time. [37]Nonlinear RF components can cause nonreciprocity. But if hardware fulfils the reciprocity the polarisations of antenna's receiving and transmitting modes should be measured. If polarisations match also, in terms of rotation, it is possible to utilize reciprocity theorem.

3.3 Array factor

Array factor (AF) is the radiation pattern obtained from antenna array which consists of N identical antennas facing to the same directions. AF is the function of the elements' complex weights and relative positions and it can be calculated with

$$AF = \sum_{n=1}^{N} w_n e^{-ikr_n}, \tag{9}$$

where w_n is complex weight applied to the signal before antenna element, r_n is relative position of the antenna element and k is the wave vector of the incident wave. [38]

The parameters of AF can be adjusted to improve the antenna array's performance. By utilizing Taylor synthesis to the complex weights of the AF we can adjust the amplitude distribution over the antenna elements. In uniform amplitude distribution, the same weighting is applied to every antenna element within that antenna array. The Taylor distribution is an optimum compromise between main lobe's width and side lobes' power level. By implementing Taylor distribution, we can decrease the power levels of side lobes with the loss of main lobe directivity. Sidelobe reduction is also called tapering. The main purpose of tapering is to reduce the inter-beam interference. [38][39]In Fig. 12 is shown how tapering effects on main lobe and side lobes and it can be seen that with tapering the side lobes are reduced, but the Half Power Beam Width (HPBW) of the main lobe increases.

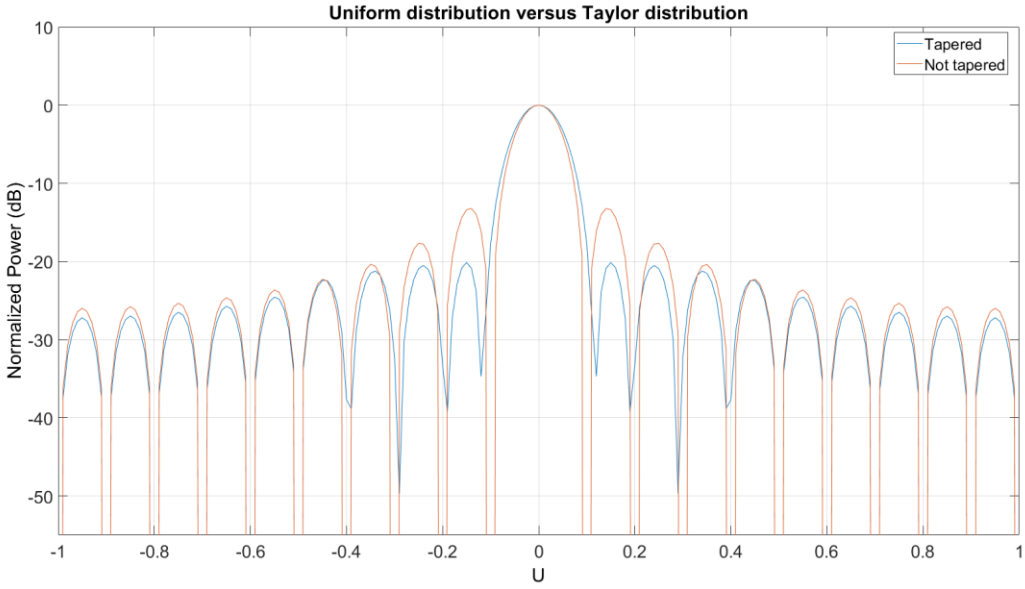

Figure 12. Uniform distribution (orange) vs Taylor distribution (blue)

3.4 Polarization

When we talk about polarization in antenna technology, it describes an electromagnetic wave that is emitted or received by an antenna to or from certain direction. Polarization is described by the antenna axis ratio, rotational speed, and tilt angle. The polarization of the radiated energy varies with respect to the center of the antenna. It can also be of different sizes in different parts of the radiation pattern. The polarization of an antenna is determined by its electric field. We can obtain information about polarization by studying the signal's electric field propagation pattern. With the obtained information we can sort the polarization into either linear, circular, or elliptical polarization.

Polarization is linear if the electric field vector travels linearly in the desired direction as a function of time. When the polarization is circular, the electric field vector travels in a circular path in its direction of propagation, and the polarization is elliptical as it travels in an elliptical path. The polarization of the circle as well as the elliptical shape can be polarized either left or right-handed. If a circularly or elliptically polarized electric field vector rotates clockwise it is right-handedly polarized, and when the vector only rotates counter clockwise it is left-handedly polarized. [40]The orientation of the linearly polarized antenna array shown in Fig. 13 is a) horizontally / vertically and b) ± 45 degrees.

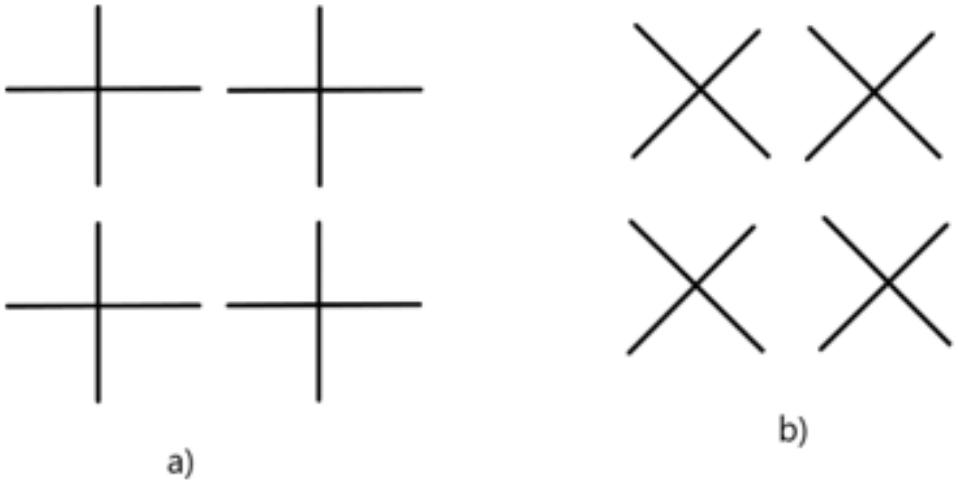

Figure 13. The orientation of the linearly polarized antenna array a) horizontally/vertically b) ± 45 degrees

Antennas which are oriented like in Fig. 13 a) are called as dual polarized antennas and antennas which are oriented like in Fig. 13 b) are referred dual slant antennas. Dual slant antennas are mostly used in FR1 because both polarizations experiences almost equal path loss and scattering in low frequencies. On the other hand, dual polarized antennas' antenna elements experiences very different scattering at low frequencies. Because of the nature of the signal propagation in the medium the horizontal polarization experiences stronger path loss than vertical polarization. Due this, the dual polarized antennas are more commonly used in FR2 bands where the LOS component is dominant, and the attenuation caused by scattering is small. Unlike FR2 bands, the FR1 bands do not require LOS component and they can utilize scattering components which makes dual slant antennas better choice to provide better coverage for low frequencies. [40]

When we are testing the DUT it is crucial to know the polarizations of antennas. Without this knowledge we cannot analyse the signal transmitted from DUT or we cannot analyse if the DUT is receiving signal correctly. In this thesis work we use DUT which operates in FR1 and thus it uses dual slant antennas.

3.5 Beamwidth

Beamwidth is one of the most important parameters in antenna measurements. The most common measured parameters are half-power beamwidth (HPBW) and first-null beamwidth (FNBW). These parameters provide information on the angular differences of the main lobe. HPBW measures the angle between the half-power points of the main lobe, i.e. -3dB points, in relation to the peak effective radiated power of the main lobe. FNBW again measures the angle between the first nulls of the radiation pattern. [41]HPBW and FNBW are presented in Fig. 14.

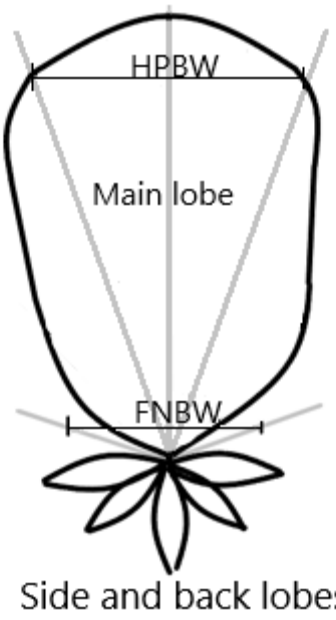

Figure 14. HPBW and FNBW measurements.

Beamwidth can be also measured with different values than with half-power. It depends on what we want to measure, but it is not very common. [22]

3.6 Efficiency, Directivity, Gain and VSWR

Efficiency of an antenna measures how well the antenna is built and matched. It measures the losses at the input terminals and losses which occurs due to the structure of the antenna. These kinds of losses can be reflection caused by mismatch between transmission line and the antenna and losses caused by conduction and dielectric characteristics of the antenna. The overall efficiency can be expressed as

$$e_0 = e_r e_c e_d, \tag{10}$$

where e_0 is the overall efficiency, e_r is the reflection efficiency, e_c is the conduction efficiency and e_d is the dielectric efficiency. By multiplying e_c and e_d we get antenna radiation efficiency e_{cd} which is used to relate the gain and directivity. [22]

In the IEE Standard Definitions of Terms of Antennas the directivity of an antenna is defined as follows: "The ratio of the radiation intensity in a given direction from the antenna to the radiation intensity averaged over all directions." [42]For isotropic source the value of directivity is 1 since the radiation intensity is equal all over the radiation pattern. The directivity can be calculated for both polarizations separately and together. The directivity for both polarizations can be presented in mathematical and is written as

$$D = \frac{U}{U_0} = \frac{4\pi U}{P_{rad}}, \tag{11}$$

where D is directivity, U is radiation intensity of specified direction, U_0 is radiation intensity of isotropic source and P_{rad} is total radiated power. From equation 11 it can be said that the directivity is ratio of radiation intensity of non-isotropic source in desired direction over that of an isotropic source. In the equation 11 the radiation intensity U is maximum intensity of radiation pattern when direction is not specified. [22]

The directivity for only one polarization is called partial directivity and it is mathematically expressed for both polarizations separately as

$$D_\theta = \frac{4\pi U_\theta}{(P_{rad})_\theta + (P_{rad})_\varphi}, \tag{12}$$

$$D_\varphi = \frac{4\pi U_\varphi}{(P_{rad})_\theta + (P_{rad})_\varphi}, \tag{13}$$

where D_θ is directivity in a given direction for θ field component, D_φ is directivity in a given direction for φ field component, U_θ is radiation intensity in a given direction for θ field component, U_φ is radiation intensity in a given direction for φ field component, $(P_{rad})_\theta$ is total radiated power in θ field component, $(P_{rad})_\varphi$ is total radiated power in φ field component. From equations above it can be defined that the partial directivity is the ratio between radiation intensity in the given direction for one field component and total radiated power for both field components. It is also true that the total directivity is the sum of partial directivities of two orthogonal polarizations.

$$D = D_\theta + D_\varphi \tag{14}$$

Higher the directivity is the higher amount of radiated power is concentrated to the given direction which results to narrower beam and higher gain. By studying heatmap in case of beam which has high directivity, we can see higher amount of power concentrated to smaller area than what we would see in case of beam which has low directivity. [22]

The gain and the directivity of the antenna are close to each other as both measures the antenna's behaviour in terms of power in certain direction. The difference between these two parameters is that as directivity only takes in account the directional properties of an antenna, the gain also considers the efficiency of an antenna. The gain is defined as the ratio of the intensity, in a desired direction, to intensity that would be observed if the power accepted by an antenna would radiate isotropically. The radiation intensity which corresponds to the isotropic radiation intensity is equal to input power divided by 4π. The gain can be mathematically expressed as

$$G = 4\pi \frac{U}{P_{in}}, \tag{15}$$

where G is the gain of the desired direction, P_{in} is the total input power and U is the radiation intensity to the desired direction. The equation 15 can deducted to more simply form where the relativity of antenna radiation efficiency and directivity is visible more clearly and it is expressed as,

$$G = e_{cd}D, \tag{16}$$

where e_{cd} is the antenna radiation efficiency. As in case of directivity, if the direction is not specified the G is the maximum gain of the radiation pattern.[22]

Voltage Standing Wave Ratio (VSWR) measures how efficiently the signal is transmitted from the source through a transmission line to an antenna. The value for VSWR is always positive and its minimum value is 1 and can be anything up to +∞. The lower the value the better is the outcome. In ideal situation the value for VSWR is 1 which means 100% of the signal's power is transmitted to the antenna. This is impossible and there will always be some sort of mismatch between antenna and transmission line which causes some of the signal's energy to be reflected to the source. Usually, the impedance matching is done to 50-Ohms, and this is the case with our antenna also. [43]

VSWR affects to the antenna radiation efficiency and thus it affects to the gain. The antenna radiation efficiency considers the loss occurred in the antenna as it is shown in the equation

$$e_{cd} = \frac{P_{rad}}{P_{in}} \tag{17}$$

If the VSWR is 5.83 it corresponds to 3.01 dB return loss which indicates that half of the incident power is reflected. Thus, the value for P_{rad} and the antenna radiation efficiency decreases and furthermore causing lower gain. [44][45]

3.7 Beam sets

In multiple SSB transmission case, the different SSBs are transmitted to air interface via their own beam. These beams are called as SSB beams and the set of multiple SSB beams is called as beam set. Different beam sets can contain different number of beams and they can have different radiation pattern. By changing the horizontal and vertical angles of the beams within the beam set we can achieve the desired radiation pattern. As it is shown in Fig. 15, the vertical angle (θ) is calculated from the norm of horizontal plane. This means that when the beam is facing straight to the direction where antenna is facing its vertical angle is 90 degrees.

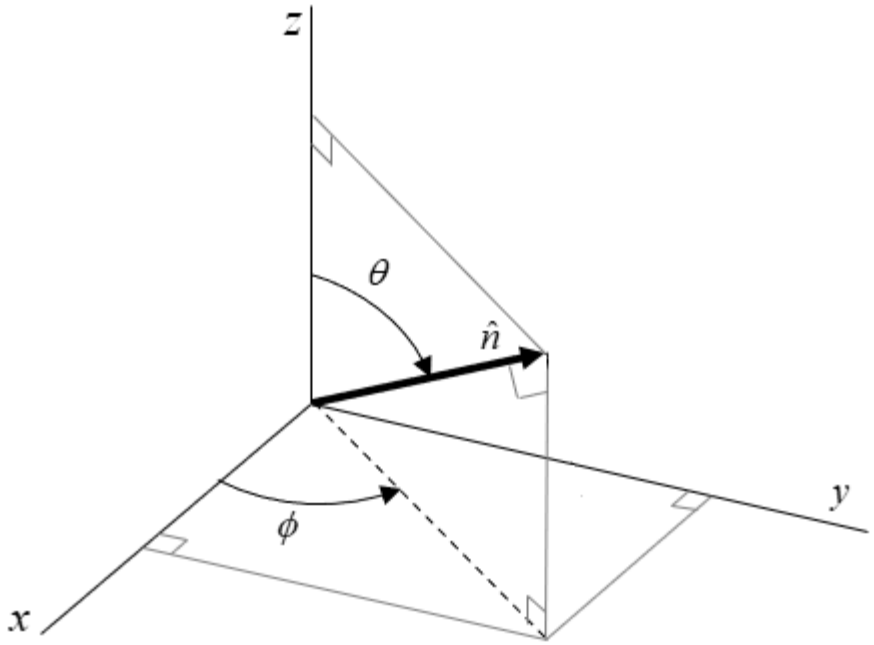

Figure 15. Horizontal (ϕ) and vertical (θ) angles of the SSB beam where the antenna is facing in the direction of the x line.

For example, with beam set #6 we have six beams with same vertical angle but with different horizontal angle. With beam set #4#4 we can have for example eight beams with same horizontal angle but four of those beams has lower vertical angle than 90 degrees and four beams with higher vertical angle than 90 degrees. With this beam set we get wider coverage on the vertical plane but more narrow coverage on the horizontal plane than with beam set #6. On the Fig. 16 is illustration of the radiation pattern of beam set #6 and beam set #4#4. The beam indexing starts from the first beam on the right which is also the first received SSB beam in time domain. In our heatmap we can conclude that the direction of the beams are as expected if the results follows the indexing shown in Fig 16.

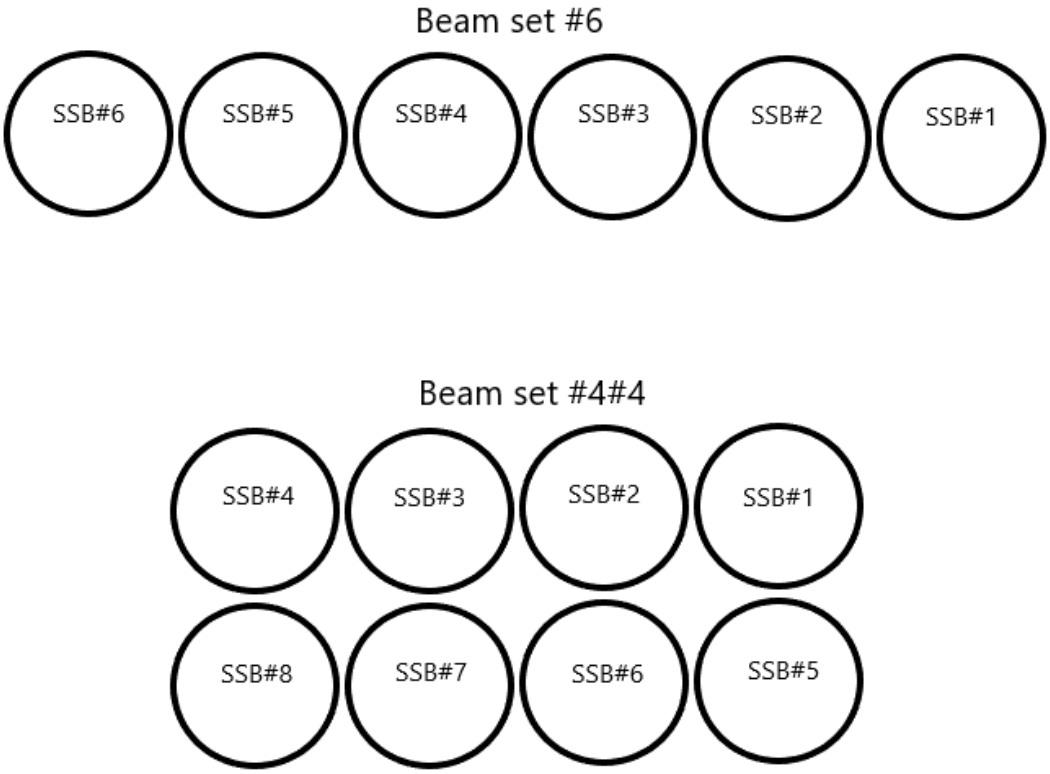

Figure 16. Illustration of beam set #6 and beam set #4#4 with beam indexing

The opening angle, which defines how widely the beams are spread, of the beam set can also vary and it can be configured for different purposes. With higher opening angle we get higher coverage but with the cost of the directivity.

4 MEASUREMENT SYSTEM AND CONTROL TOOL

The most important parts of the measurement system are the anechoic chamber, RF-switch, spectrum analyser and the antennas which we use to measure the power level of the SSB beams. In this chapter we will study all these objectives and finally we study how we control this system.

4.1 Anechoic Chamber

Transmitting and receiving the signal is performed in OTA mode and thus it is crucial to protect the signal from any interference and prevent the signal from escaping. Such interference can be caused by for example other test lines nearby, wireless local area network (WLAN), other operators within the same band or by internal reflections where the signal under testing is reflecting inside the chamber. Also, our system can cause interference to the outside world. [46]In Fig. 17 is presented overall picture of the anechoic chamber.

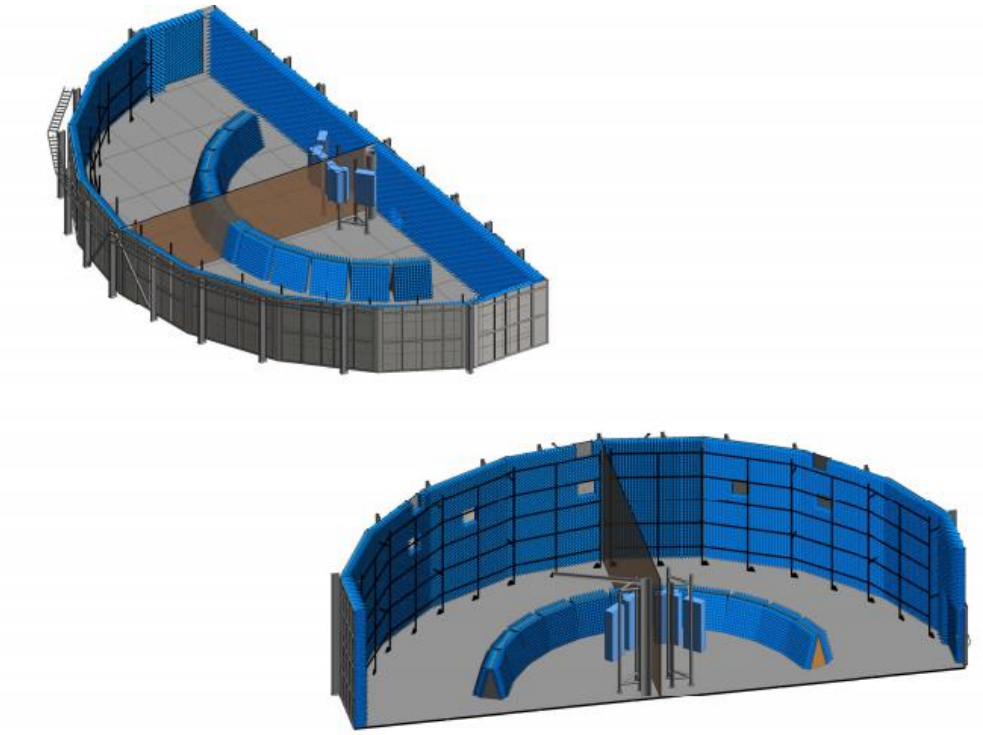

Figure 17. Anechoic Chamber

To ensure that our test environment won't cause interference to others, or the test results won't be manipulated by the interference the chamber is covered with anechoic absorber material. The purpose of absorber material is to absorb all electromagnetic waves. In our test environment we utilize pyramidal absorbers which are fabricated from urethane foam. With pyramidal absorbers the length of the absorber defines the lowest operating frequency. The lower the frequency is the longer absorber is needed. The length should be approximately one wavelength of the lowest used frequency in the chamber. [47]

We use two kinds of absorbers with the length of 18-inch and 12-inch. The 18-inch absorber is used on the wall behind the radio stand and on both side walls. The frequency usage range of this absorber is from 500 MHz to 40 GHz and its physical measures are presented in Fig. 18a). The 12-inch absorber is used on the antenna wall, ceiling and to create the shallow wall between antennas and radio stand to prevent reflections from the floor. The shallow wall is 1.2m high and 20m long. The frequency range for 12-inch absorber is from 1 GHz to 40 GHz and its physical measures are presented in Fig. 18b).

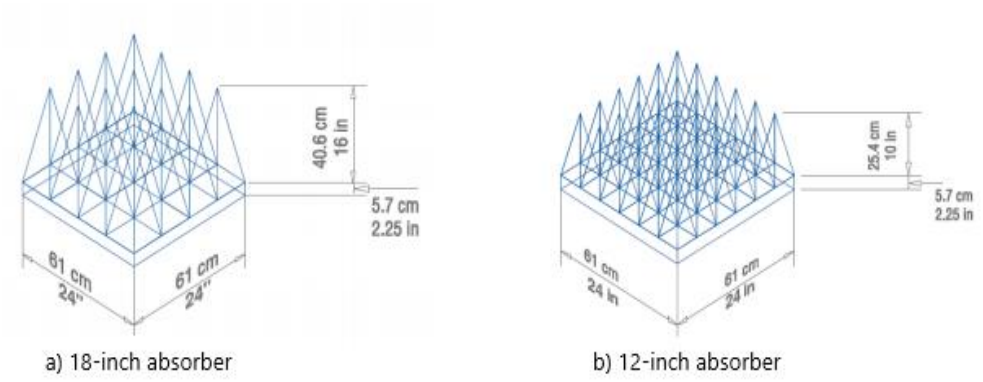

Figure 18. a) The physical size of 18-inch pyramidal absorber. b) The physical size of 12-inch pyramidal absorber.

The chamber consists of two sectors. From Fig 17. we can see that on the middle of the chamber lies curtain which reaches from back of the chamber to the curved wall and from the ceiling to the floor. This curtain is called as shielded curtain which will attenuate signals which operates from 1 MHz to 18 GHz about 60 dB. Both sectors are identical but as mirror images of each other. On the Fig 19. is visible left sector of the chamber.

Figure 19. Left sector of the chamber

4.2 The measurement equipment

The conventional OTA measurement system is built on: antennas, which receive and feed the signal, and analyser which performs measurements and analyses the signal. Our system is more complex and during this chapter we will go through the hardware of our measurement system.

4.2.1 Antennas

From radio stand's point of view on the opposite wall of the chamber is the antenna grid. The antenna grid is drawn in black to the curved wall on the Fig. 17. This composite rail grid structure has 18 vertical rails and 5 horizontal rails and has total 40 positions for the antennas. On this test environment we have in total 32 antennas in use, but per sector 16 antennas as the chamber consists of two sectors. We use Dual Polarized Vivaldi Antennas (DVPA) which operating frequency range is from 700 MHz to 6000 MHz. The physical size of the antenna is 72mm x 100mm x 1mm. The VSWR of the antenna in the function of frequency for both polarizations are presented in the Fig. 20.

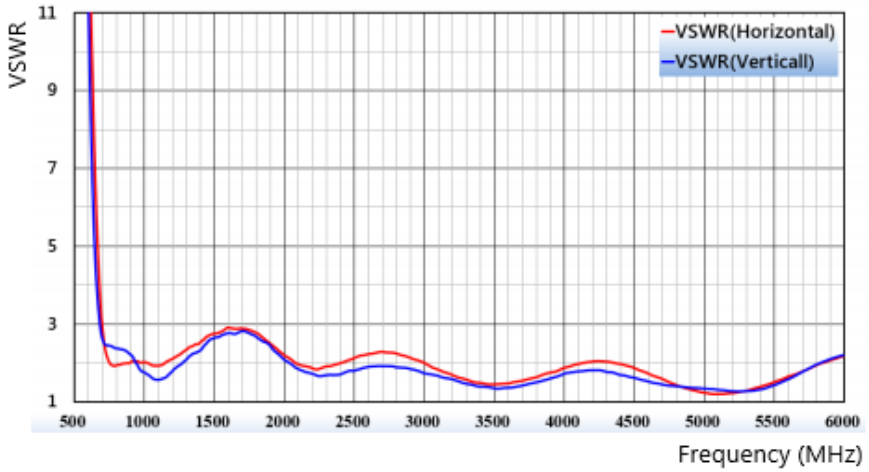

Figure 20. VSRW of the DVPA for vertical (blue) and horizontal (red) polarizations.

As it is visible from Fig 20. the value of VSWR is indeed below 3 for both polarizations within the operating frequency range of the DVPA i.e. from 700 MHz to 6000 MHz.

4.2.2 Spectrum analyser and Vector Signal Analysis

In order to capture the signal received by the antennas we need spectrum analyser (SA). On this thesis we utilize Keysight Infiniium MXR-Series spectrum analyser. The SA has in total eight channels and it can operate in frequencies between 500 MHz to 6GHz. This means that we can measure and analyse the signal from eight different antennas simultaneously.

After the signal is captured, we need to perform the desired measurements. The analysis and measurement can be done also with SA itself, but to have more convenient and versatile way to do it we use Vector Signal Analysis (VSA) 89600 tool. The VSA is an application installed on remote PC which is used to control the SA and analyse the signal. The VSA communicates with SA through TCP/IP socket connection. The VSA tool is also crucial for programming.

4.2.3 RF-switch

On the antenna grid lies 32 DVPA antennas, but on the SA we have only 8 ports for RF cables. This points out new challenge: How we can seamlessly perform the desired measurements for the signal from desired antennas without changing the cabling between SA and the antennas? The solution is RF-switch.

The RF-switch has in total 32 input ports and 16 output ports. It consists of four parts where each part has equal amount of input and output ports. The antennas on the wall are connected to the input ports and the SA's channels are connected to the output ports. The coupling of our measurement system is drawn into Fig. 21.

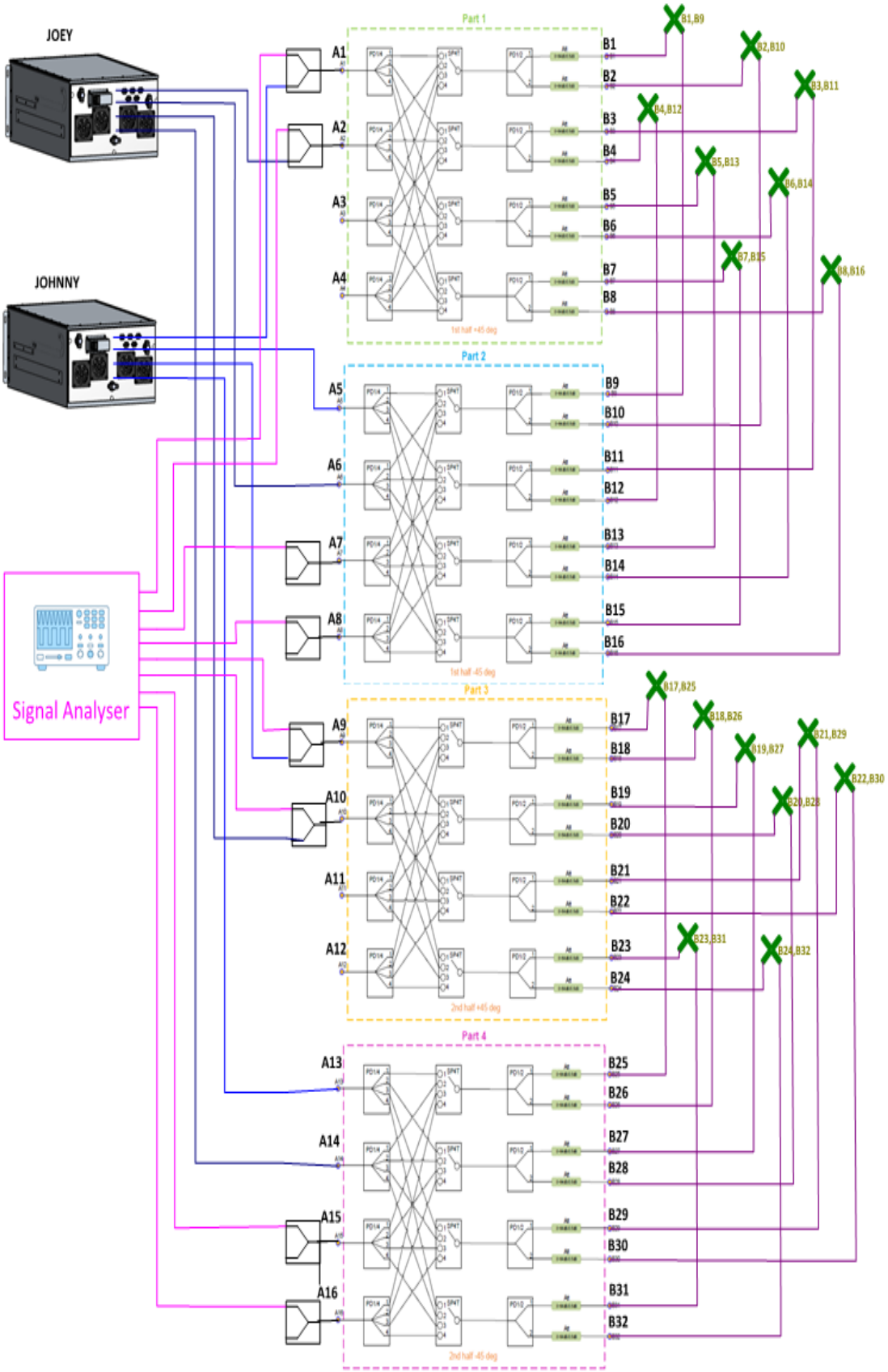

Figure 21. The coupling of the measurement system

On the right side of Fig. 21 are antennas (green tabs) and on the left side is the SA. “Johnny” and “Joey” represents UE simulators. As it is visible the eight channels of the SA are connected to the output ports (A1 – A16) and antennas are connected to the input ports (B1 – B32) of the RF-switch. It is also possible to use power dividers to take the signal to the UE simulators simultaneously. The RF-switch itself consists of four identical parts. Part 1 includes the ports A1 – A4 and B1 – B8, part 2 includes the ports A5 – A8 and B9 – B16, part 3 includes the ports A9 – A12 and B17 – B24 and part 4 includes the ports A13 – A16 and B25 – B32. The different polarisations of antennas are allocated to the different parts of the RF-switch. Part 1 and part 3 contains the +45-degree polarisations of the antennas and part 2 and part 4 contains the -45-degree polarisation.

The parts consist of splitters and programmable switches and attenuators. Each input port has its individual programmable attenuator. It is important to notice that the input ports forms pair. For example, ports B1 and B2 are connected to the same switch through the same splitter and hence they form a pair. This means that if we want to measure the signal received by the antenna which is connected to port B1 we need to attenuate completely the B2. Each part has four switch and each switch’s output port is connected to each output port of the part. Hence, it is possible to connect each output port to each input port within the same part.

4.3 Implementation of the OTA measurement system

On this thesis I implemented a Python code which is used to control the whole measurement system all the way from antennas to the VSA. On Fig. 22 is flow chart which presents the main steps of the code

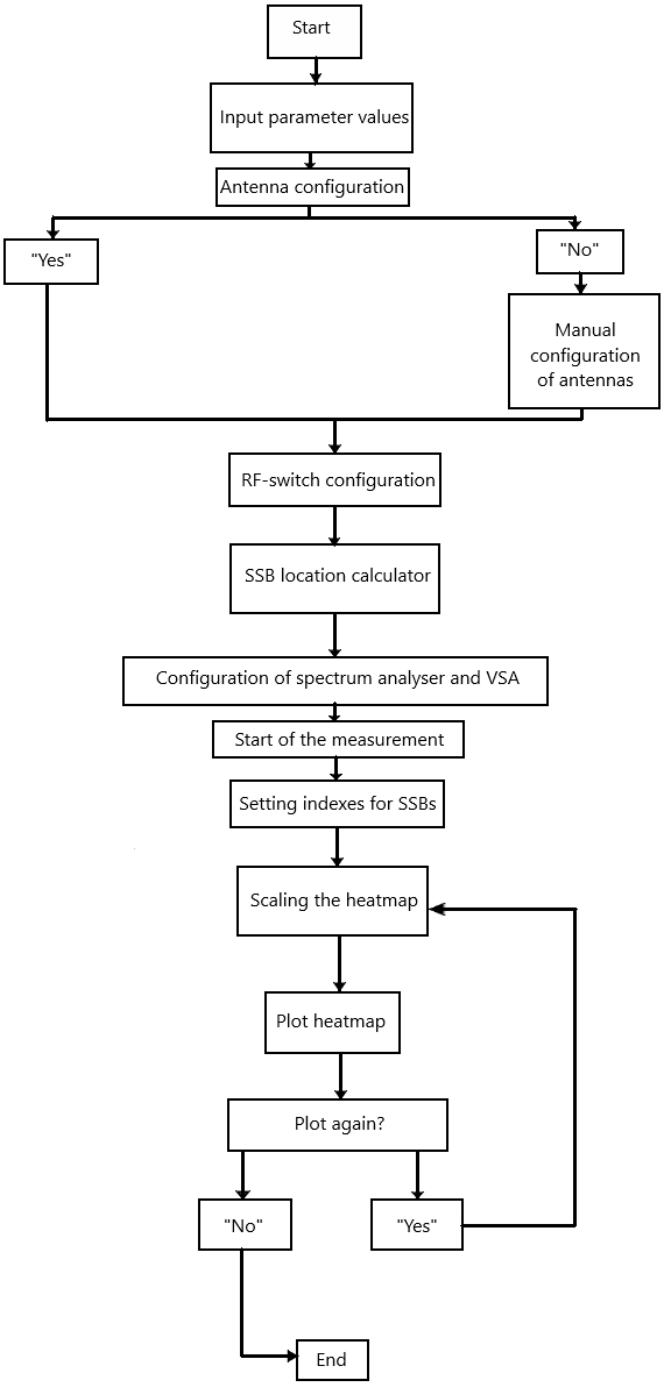

Figure 22. Flow chart of the code

On the first step the code asks from the user the mandatory parameter values for the code. These are center frequency, SSB frequency, bandwidth, PCI, SSB periodicity, number of transmitted SSBs, SCS and SSB SCS. The center frequency, PCI, SSB periodicity, bandwidth, and number of transmitted SSBs are used for basic configuration of SA and VSA. Bandwidth, SCS and SSB SCS are used as input variables for SSB location calculator which is introduced in more detail later.

On the second step the code asks if the user wants to use the default antennas in the measurement. The default antennas contain eight antennas which are all allocated to x-axis of the antenna grid with even spacing. If user answers "yes" the default antennas will be used, but if the answer is no the code asks from the user to manually input the desired antennas and their ports.

On the third step of the code happens the configuration of the RF-switch. The center frequency will be set as defined on the first step and the input and output ports of the RF-switch will be connected as defined on the second step. All other paths will be completely attenuated.

On the fourth step is calculator for SSB location in frequency domain. This calculator takes input values from bandwidth, SCS and SSB SCS. The output of the calculator is RBOffset and kSSB which will be then configured to the VSA. It is crucial to successfully calculate the SSB position to detect the SSB power correctly. The calculator calculates firstly the lowest frequency of the SSB as follows

$$f_{SSBLow} = f_{SSB} - (10 * 12 * SSBSCS), \tag{18}$$

where f_{SSBLow} is the lowest frequency of the SSB and f_{SSB} is the frequency of the SSB. Then the calculator checks if the SCS is 30 kHz or 15 kHz. If the SCS is 30 kHz the offset will be calculated with equation 19 as

$$Offset = \left(\frac{N_{RB} - f_c - f_{SSBLow}}{BW_{RB}}\right) * 2, \tag{19}$$

where f_c is the center frequency and BW_{RB} is the bandwidth of one resource block. If SCS is 30 kHz the offset needs to be multiplied with value 2 to get the offset match up to 15 kHz SCS as the VSA assumes the offset always in 15 kHz scale. If the SCS is 15 kHz the offset will be calculated with equation 20.

$$Offset = \frac{N_{RB} - f_{SSBLow} - f_c}{BW_{RB}} \tag{20}$$

After the offset is calculated the RBOffset and kSSB can be achieved with modulo operation. By executing the modulo operation to offset, the integer equals to RBOffset and with the remainder we can calculate the kSSB with equation 21 as

$$kSSB = \frac{\mathrm{r} * 180\,\mathrm{kHz}}{15\mathrm{kHz}}, \tag{21}$$

where r is the remainder.

After the configuration of the SA and VSA is completed, we proceed to the sixth step which is triggering the measurement. On the seventh step all the SSBs are detected by VSA and based on the number of the transmitted SSBs VSA will set indexing of the SSBs.

On the eight step the code will ask from the user what kind of scaling is going to be used. The default is from -80 dBV to -40 dBV, but user can choose whatever scaling he decides to use. On the nineth step will happen the plotting of the heatmap

itself and user will see the results of the measurement and begin the analyses. After this user can choose to either plot the heatmap again and choose either same or different scaling for the plot or just end the code.

5 MEASUREMENTS RESULT ANALYSIS OF SELECTED RF PARAMETERS

On this chapter we will go through the measurement results of the OTA measurement system. We made three measurements with same RU but with different beam sets. Measurements were executed several times for the same beam set to ensure the stability of the system. The RU in use has 64 antenna elements and operates in FR1 band 41 with center frequency of 2639.43 MHz. Measurements were executed with beam set 2, 4 and 6. All measurements contains power received by antennas for each SSB where the first SSB power measurement is in the top bar and the last SSB power measurement is in the bottom bar. All measurement antennas were located on the horizontal plane of the antenna grid. The antenna indexes are on the x-axis of the bars and goes from left to right. The indexing of the SSBs starts from the 1 and the indexing of the measurement antennas starts from the 0. In every measurement result there is also colour bar on the right side of the figure which describes the relation between the power and colour. On the Fig. 23 is visualized the allocation of the measured antennas on the wall.

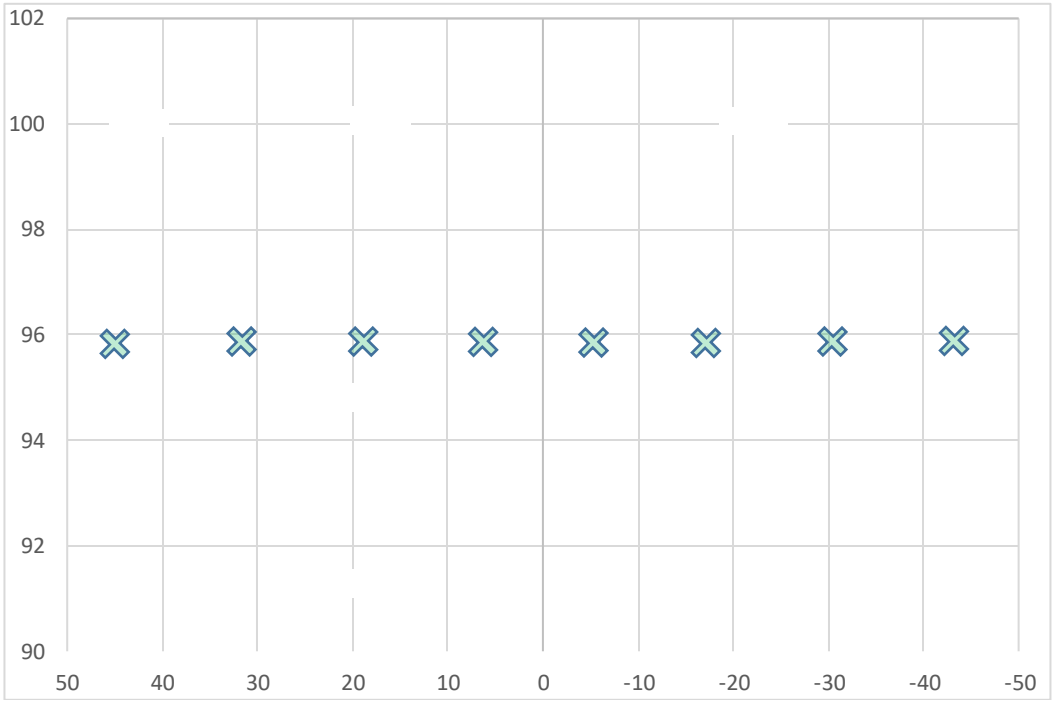

Figure 23. Allocation of the measured antennas on the sector with the vertical and horizontal degrees.

5.1 Measurement results for beam set 2

The first measurement was executed with beam set 2. The measurement result is visible in Fig. 23.

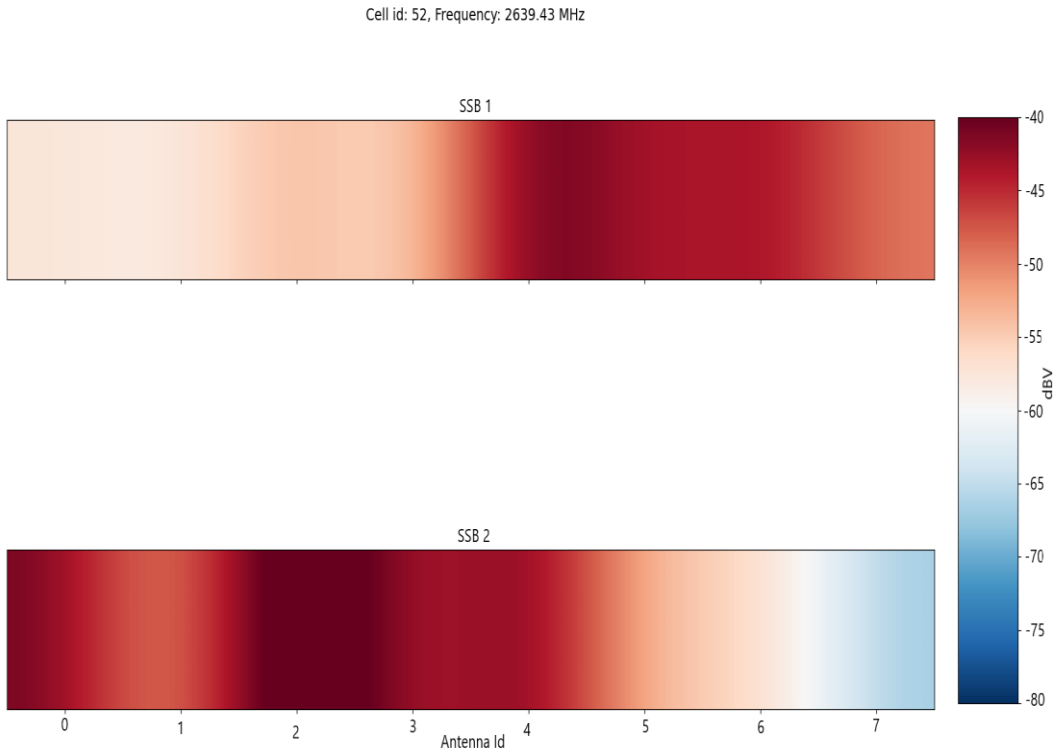

Figure 23. Measurement result with beam set 2.

By observing measurement results in Fig. 23 we can see that the direction of the SSB beams is as expected. The first SSB beam is located on the right side of the sector and the second SSB beam on the left side of the sector. Also, as it is visible in the Fig. 23 the HPBW of both beams are wide enough to cover the whole sector. Between the SSB beams there is no power drop visible. This ensures that UE can seamlessly change the SSB beam if it is moving from beam to another. This can be concluded as the high power of the beams are measured from antenna 0 to 4 for SSB beam 2 and from antenna 4 to 7 for SSB beam 1.

By comparing the powers received from SSB 1 and SSB 2 we can see that the SSB 2 has slightly wider beam and higher power at the direction of the main lobe and slightly lower power at the direction of the side lobes. From this we can conclude that the directivity and positioning of the SSB beam 2's main lobe is more accurate than with the SSB beam 1.

It can be also seen that the power received from SSB 2 has minor drop of the power at the location of antenna id 1 and minor increase of the power at the location of antenna id 0. It seems that this RU has minor beamforming issue with this beam set. The power of the main lobe should be continuous all over within the beam without unexpected power drops.

5.2 Measurement results for beam set 4

On the second measurement we used beam set 4. The results are visible in Fig. 24.

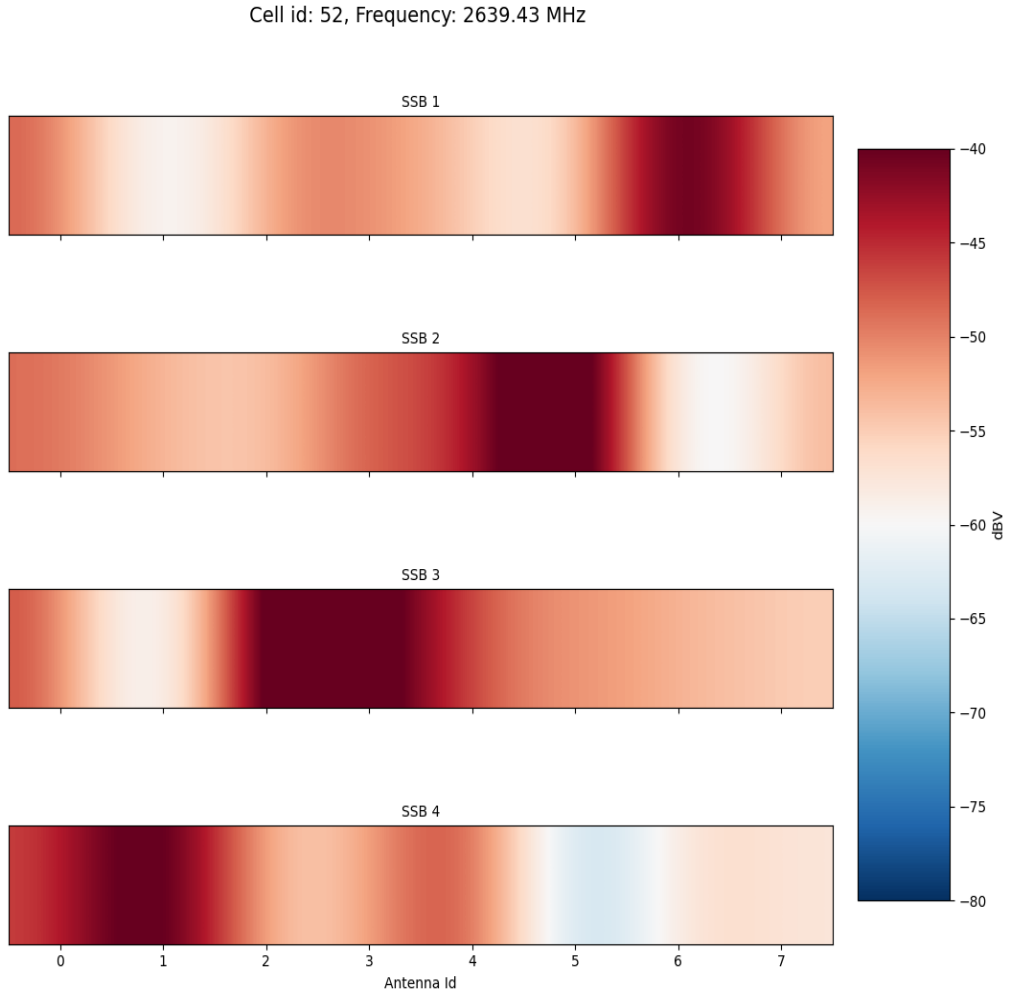

Figure 24. Measurement result with beam set 4.

From Fig. 24 we can also conclude that all SSB beams are formed and the direction of the SSB beams is as expected. The first SSB beam is on the right side of the sector and the last SSB beam on the left side of the sector. The allocation of beams is as expected, and the beams cover the whole sector without leaving any empty space between. However, there is slight decrease of the SSB power between the beams which is not ideal situation as the SNR will decrease when the UE is moving from beam to another. The HPBW of each beam is considerably smaller than with beam set 2. This can be observed as the high-power region of each SSB beam covers one and slightly more than two antennas. As the number of beams increases there is no need for as wide beams to cover the whole sector. As it is concluded in chapter 3.6 the directivity increases when the beamwidth decreases.

This is also visible in the measurement results. As with the beam set 2, we can see also here that the SSB power level with SSB 1 is slightly lower than with the other SSB beams. The RU seems to have minor issue with beamforming to that direction. The SSB 4 has good power level on antenna id 1 and as the antenna id 1 with beam set 2 had slightly more poor power level than other antennas, we can exclude that the error with beam set 2 would be error in measurement system.

5.3 Measurement results for beam set 6

On the third measurement we used beam set 6 which was the highest possible number of beams with our operating center frequency. The results of the third measurement are visible on the Fig. 25.

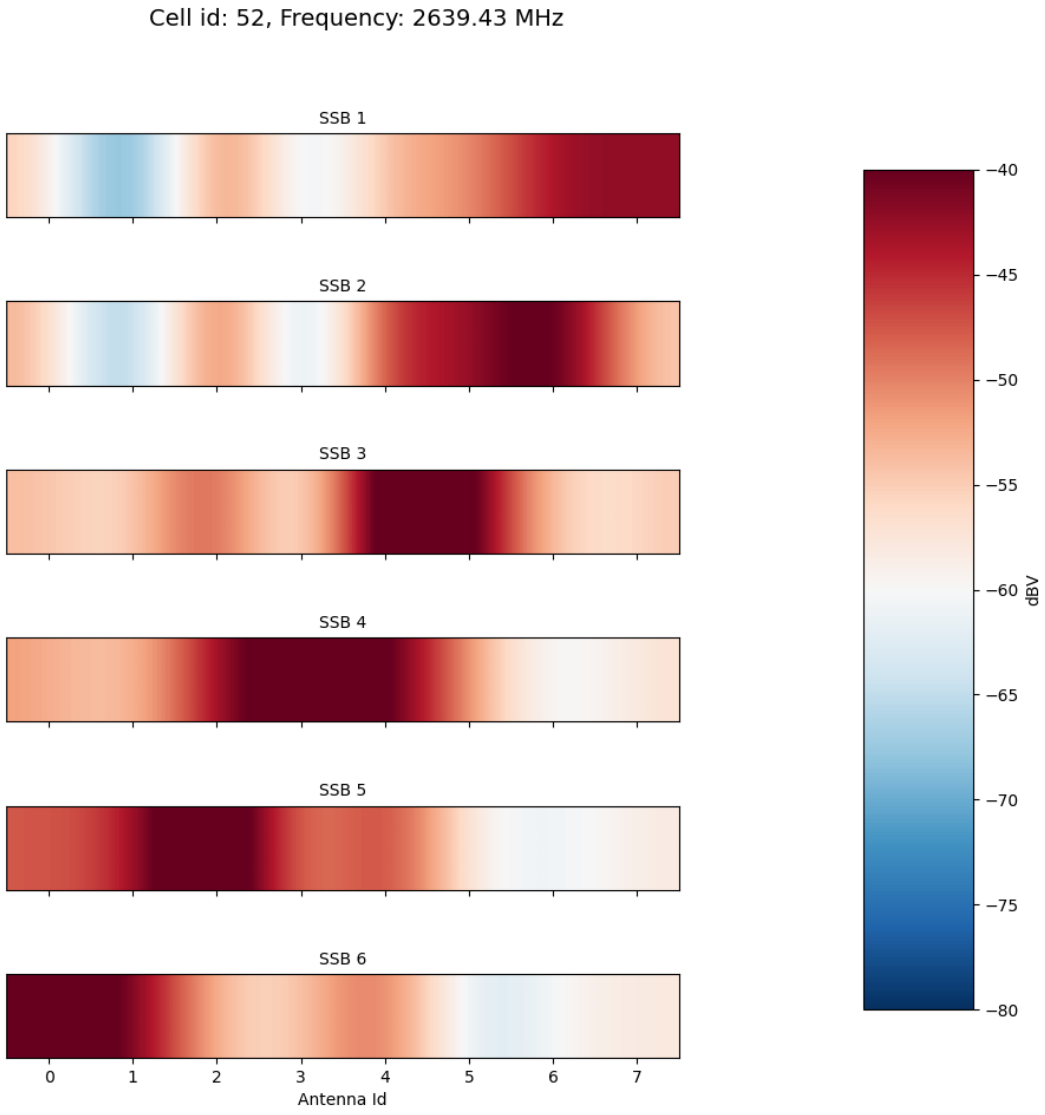

Figure 25. Measurement result with beam set 6.

As with the previous measurement results, it can be concluded that all SSB beams are visible, and the directions of the beams are as expected. The power levels between the beams are approximately equal. Only SSB beam 1 seems to have slightly lower power level. The allocation of the SSB beams is better than with beam set 4 as there is no drop in power levels between the beams. The HPBW of the beams are approximately the same as with beam set 4 and thus is the directivity. As the HPBW remains constant, but the number of the SSB beams increases, the coverage of the radiation pattern also increases. This can be also observed from the Fig. 25 as the beams are more closely spaced within the sector and the high-power region is seamlessly visible from antenna id 0 to antenna id 7.

6 CONCLUSIONS

The measurement results brought us valuable information about the RU's beamforming capabilities. They also showed us differences between different number of transmitted SSB beams i.e. beam sets. In all measurements all SSB beams were visible, and the direction of the beams were as they should be. Overall, all beams had the approximately same power level despite SSB beam 1 had minor decrease of power in all measurement results. From this we can conclude that our DUT has issues with beamforming SSB beam 1 with any beam set. There were also differences in measurement results between beam sets.

With beam set 2 we had the highest HPBW. This is as expected as the number of the beams is lowest. The beam widths were wide enough to cover the whole sector. However, there was minor error in SSB beam 2 in the location of antenna id 1. By comparing the power measured by antenna id 1 in other measurement we can conclude that this RU has problems with beamforming the second beam with beam set 2.

With beam set 4 the HPBW of the beams were narrower than with beam set 2. This behaviour was expected as the need for wider beams decreases when the number of beams increases. The spacing between SSBs were slightly too wide as there was minor decrease of power visible between different beams

With beam set 6 the HPBW was same as with beam set 4 but the SSBs were allocated more closely to each other. Also, the coverage was slightly better than with beam set 4 or beam set 2. There was no power dropping visible within the SSB beams.

Overall, the beamforming of this RU works as expected and it can be taken in use for other testing purposes. There was no major issues or differences between different beam set in terms of functionality. However, the beam set 6 seems to be working the best and based on these measurements that would be the most suitable choice as it has the highest coverage with the most stable performance.

7 SUMMARY

In the master thesis I successfully managed to implement Python code to control whole OTA measurement system. The Python code was able to control all devices from the antennas to the VSA. There were no issues visible either on the SSB location calculator. We managed to get reliable measurement results about the RU's BF capabilities with multiple different beam sets. The measurement results showed us that the RU had some minor problems with BF. The radiation patterns of different beam set were as expected but the SSB beam 1 had slightly lower power on all the measurements. Also, with beam set 2 there was an unexpected decrease of power on the SSB beam 2 in the location of the second antenna. This issue was not visible with other beam sets. The measurements proved that the RU's BF capabilities were on the expected level, and it can be taken into other testing. Based on the measurement results the beam set 6 seemed to be the best choice for testing which requires high stability and great coverage. The beam set 4 would also be good choice but its coverage was slightly worse than with beam set 6.

The topic on the master thesis was very interesting and it gave me a better chance of learning to code with Python. It showed me that basically anything can be programmed if needed. The thesis also taught me more about the importance of OTA testing. The performance of techniques like mMIMO or BF cannot be reliable measured without OTA testing. Thesis gave me also different point-of-view as I could see the location of SSBs visualised rather than analysing them from the time domain on the spectrum analyser.

8 REFERENCES

[1] 3GPP (2021), LTE, (accessed 22.01.2021) https://www.3gpp.org/technologies/keywords-acronyms/98-lte

[2] Ghayas, A. (13.9.2019), What is the difference between GSM, UMTS and LTE, Commsbrief, Article, (accessed 22.01.2021) https://commsbrief.com/difference-between-gsm-umts-lte/

[3] Real Wireless Ltd (27.1.2011), 4G Capacity Gains, Report, (accessed 22.01.2021) https://www.ofcom.org.uk/__data/assets/pdf_file/0038/74999/4gcapacitygainsfinalreporta1.pdf

[4] Decreusefond, L. & Ferraz, E. & Martins, P. & Vu, T.T. (April 2012), Robust methods for LTE and WiMAX dimensioning, ResearchGate

[5] Arimas, LTE Guard Band Calculation, https://arimas.com/2016/09/02/lte-guard-band-calculation/

[6] CableFree, FDD vs TDD Technology, (accessed 13.02.2021) https://www.cablefree.net/wirelesstechnology/fdd-vs-tdd/

[7] Munir, A. (10.6.2020) BATTLE OF THE BANDS, FDD vs TDD, Radio Tech Corp., (accessed 13.02.2021) https://www.radiotechcorp.com/battle-of-the-bands-fdd-vs-tdd/

[8] Garg, V. K. (2007). *Wireless communications and networking* (1st edition.). Amsterdam; Boston: Elsevier Morgan Kaufmann.

[9] Hatahet, A. & Jain, A (2018) Beamforming in LTE FDD for multiple Antenna Systems, Department of Electrical and Information

[10] Parkvall, S. & Dahlman, E. & Furuskär, A. & Frenne, M. (2017) NR: The New 5G Radio Access Technology

[11] Stewart J. (2014) 5G will require new as well as established spectrum bands, but the availability of new bands is not confirmed, Analysis Mason, Article, (accessed 18.02.2021) http://www.analysysmason.com/AboutUs/News/Newsletter/5G-spectrum-Oct2014/

[12] Mumtaz S., Rodriguez J. & Dai L. (2017) mmWave Massive MIMO: A Paradigm for 5G. Academic Press, 1-1.2.

[13] Electronics notes, LTE Frequency Bands, Spectrum & Channels, (accessed 18.02.2021), https://www.electronics-notes.com/articles/connectivity/4g-lte-long-term-evolution/frequency-bands-channels-spectrum.php

[14] Erik Dahlman, Stefan Parkvall, Johan Skold, 5G NR: The Next Generation Wireless Access Technology, Academic Press, 9.8.2018

[15] Kumara S., How LTE Stuff Works?, (accessed 10.04.2021) http://howltestuffworks.blogspot.com/2019/10/5g-nr-synchronization-signalpbch-block.html

[16] Z. Lin, J. Li, Y. Zheng, N. V. Irukulapati, H. Wang and H. Sahlin, "SS/PBCH Block Design in 5G New Radio (NR)," *2018 IEEE Globecom Workshops (GC Wkshps)*, Abu Dhabi, United Arab Emirates, 2018, pp. 1-6, doi: 10.1109/GLOCOMW.2018.8644466.

[17] Sharetechnote, 5G/NR - SS Block, (accessed 10.04.2021), https://www.sharetechnote.com/html/5G/5G_SS_Block.html

[18] Sharetechnote, 5G/NR - FR/Operating Bandwidth, (accessed 12.10.2021), http://www.sharetechnote.com/html/5G/5G_FR_Bandwidth.html#38_101_1_Table_5_3_2_1
[19] Sharetechnote, 5G/NR - Resource Block Indexing, (accessed 12.10.2021) https://www.sharetechnote.com/html/5G/5G_ResourceBlockIndexing.html
[20] David Tse, Berkeley Pramod Viswanath, Fundamentals of Wireless Communication, Chapter 3, 10.9.2004
[21] Mathuranathan Viswanathan, August 6, 2014, https://www.gaussianwaves.com/2014/08/mimo-diversity-and-spatial-multiplexing/
[22] Balanis C. (2005) Antenna Theory: Analysis and Design, 3rd edition. John Wiley & Sons. Hoboken, New Jersey.
[23] Ngo H. Q. (2015) Massive MIMO: Fundamentals and System Designs, Linköping University Electronic Press. Chapter 1.
[24] Powell C (2014) Technical Analysis: Beamforming vs. MIMO Antennas, Radio Frequency Systems (RFS), White paper.
[25] Björnson E., Bengtsson M. & Ottersten B. (2014) Optimal Multiuser Transmit Beamforming: A Difficult Problem with a Simple Solution Structure. IEEE Signal Processing Magazine. Lecture note
[26] Osseiran A., Monserrat J. F. & Marsch P. (2016) 5G Mobile and Wireless Communications Technology. Cambridge University Press. 137-155 pp.
[27] Sohrabi F. & Yu W. (2016) Hybrid Digital and Analog Beamforming Design for Large-Scale Antenna Arrays. IEEE Journal of Selected Topics in Signal Processing 10.
[28] Panagopoulos A. D. (2015) Handbook of Research on Next Generation Mobile Communication Systems. IGI Global. 20p
[29] TechTerms, DUT, (accessed 23.04.2021), https://techterms.com/definition/dut
[30] M. Sonkki, S. Myllymäki, N. Tervo, M. E. Leinonen, M. Sobocinski, G. Destino and A. Pärssinen (2018) Linearly Polarized 64-element Antenna Array for mm-Wave Mobile Backhaul Application, EUCAP2018, pp.1-5, London, UK, Apr 9 – 13, 2018, https://ieeexplore.ieee.org/stamp/stamp.jsp?tp=&arnumber=8568683
[31] Biamp. (11.7.2020), Gain structure: input and output levels, (accessed 28.10.2021) https://support.biamp.com/General/Audio/Gain_structure%3A_input_and_output_levels
[32] Keysight, Converting dBm to dBv in a 50 Ohm System, (accessed 18.11.2021) https://edadocs.software.keysight.com/kkbopen/converting-dbm-to-dbv-in-a-50-ohm-system-588265460.html
[33] Bevelacqua, Pete. "Friis Equation - (aka Friis Transmission Formula)", (accessed 10.04.2021) www.antenna-theory.com
[34] Krishna M. B. & Mauri J. L. (2016) Advances in Mobile Computing and Communications: Perspectives and Emerging Trends in 5G Networks. CRC Press. 1.6-7
[35] L. Vallozzi, H. Rogier, in Smart Textiles and their Applications, 2016
[36] Zhimeng Zhong, Li Fa, Shibin Ge, FDD Massive MIMO Uplink and Downlink ChannelReciprocity Properties: Full or Partial Reciprocity?, 31.12.2019

[37] RF Wireless World, Coherence Bandwidth and Coherence Time, (accessed 20.5.2021) https://www.rfwireless-world.com/Terminology/Coherence-Bandwidth-Coherence-Time.html
[38] Bevelacqua, Pete. The Array Factor, (accessed 24.04.2021) www.antenna-theory.com
[39] K. Ch. sri Kavya, Y. N. Sandhya Devi, G. Sudheer Kumar, Narendra Neupane, Performance evaluation of array antennas, International Journal of Modern Engineering Research (IJMER), Vol.1, Issue.2,pp-510-515, (accessed 24.04.2021)
[40] Arto Kinos, Over the Air Beamforming Measurement Techniques with a Case Study on Crest Factor Reduction's Effect on Error Vector Magnitude. Diplomityö. Oulun yliopisto, sähkö- ja tietotekniikan osasto, Oulu.
[41] Tutorials point, antenna theory, 20.11.2019, URL: https://www.tutorialspoint.com/antenna_theory/antenna_theory_beam_width.htm
[42] IEEE Standard Definitions of Terms for Antennas. IEEE Std 145-1993, Antenna Standards Committee of the IEEE Antennas and Propagation Society, New York, USA.
[43] Data-Alliance, VSWR: Impedance Matching in Antennas & Antenna Cables. (accessed 15.8.2021) https://www.data-alliance.net/blog/vswr-impedance-matching-in-antennas/
[44] James McLean, Robert Sutton, and Rob Hoffman, TDK RF Solutions, Interpreting Antenna Performance Parameters for EMC Application: Part 1.
[45] Johnny Lienau (4.2.2019), Laird Connectivity, Understanding Antenna Design, https://www.lairdconnect.com/resources/white-papers/understanding-antenna-design
[46] Zhang Z. (2011) Antenna Design for Mobile Devices. John Wiley & Sons (Asia) Pte Ltd. IEEE Press.
[47] Huang Y. & Boyle K. (2008) Antennas: From Theory to Practice. John Wiley & Sons. pp 267-274.
[48] HBR radiofrequency technologies, LTE Frequency Bands, (accessed 18.02.2021), https://halberdbastion.com/technology/cellular/4g-lte/lte-frequency-bands
[49] 3GPP Specification – FR1 (sub 6 GHz), https://www.3gpp.org/
[50] 3GPP Specification – FR2 (mmWave), https://www.3gpp.org/

9 APPENDICES

Appendix 1 LTE frequency bands [48]

LTE frequency bands	Uplink channel	Downlink channel	Duplex Mode
Band 1	1920 MHz – 1980 MHz	2110 MHz – 2170 MHz	FDD
Band 2	1850 MHz – 1910 MHz	1930 MHz – 1990 MHz	FDD
Band 3	1710 MHz – 1785 MHz	1805 MHz – 1880 MHz	FDD
Band 4	1710 MHz – 1755 MHz	2110 MHz – 2155 MHz	FDD
Band 5	824 MHz – 849 MHz	869 MHz – 894 MHz	FDD
Band 6	830 MHz – 840 MHz	875 MHz – 885 MHz	FDD
Band 7	2500 MHz – 2570 MHz	2620 MHz – 2690 MHz	FDD
Band 8	880 MHz – 915 MHz	925 MHz – 960 MHz	FDD
Band 9	1749.9 MHz – 1784.9 MHz	1844.9 MHz – 1879.9 MHz	FDD
Band 10	1710 MHz – 1770 MHz	2110 MHz – 2170 MHz	FDD
Band 11	1427.9 MHz – 1452.9 MHz	1475.9 MHz – 1500.9 MHz	FDD
Band 12	698 MHz – 716 MHz	728 MHz – 746 MHz	FDD
Band 13	777 MHz – 787 MHz	746 MHz – 756 MHz	FDD
Band 14	788 MHz – 798 MHz	758 MHz – 768 MHz	FDD
Band 17	704 MHz – 716 MHz	734 MHz – 746 MHz	FDD
Band 18	815 MHz – 830 MHz	860 MHz – 875 MHz	FDD
Band 19	830 MHz – 845 MHz	875 MHz – 890 MHz	FDD
Band 20	832 MHz – 862 MHz	791 MHz – 821 MHz	FDD
Band 21	1447.9 MHz – 1462.9 MHz	1495.5 MHz – 1510.9 MHz	FDD
Band 22	3410 MHz – 3500 MHz	3510 MHz – 3600 MHz	FDD
Band 23	2000 MHz – 2020 MHz	2180 MHz – 2200 MHz	FDD
Band 24	1625.5 MHz – 1660.5 MHz	1525 MHz – 1559 MHz	FDD
Band 25	1850 MHz – 1915 MHz	1930 MHz – 1995 MHz	FDD
Band 26	814 MHz – 849 MHz	859 MHz – 894 MHz	FDD
Band 27	807 MHz – 824 MHz	852 MHz 869 MHz	FDD
Band 28	703 MHz – 748 MHz	758 MHz – 803 MHz	FDD
Band 29	DL only	717 MHz – 728 MHz	FDD
Band 30	2305 MHz – 2315 MHz	2350 MHz – 2360 MHz	FDD
Band 31	452.5 MHz – 457.5 MHz	462.5 MHz -467.5 MHz	FDD
Band 32	DL only	1452 MHz – 1496 MHz	FDD
Band 33	1900 MHz – 1920 MHz	1900 MHz – 1920 MHz	TDD
Band 34	2010 MHz – 2025 MHz	2010 MHz – 2025 MHz	TDD
Band 35	1850 MHz – 1910 MHz	1850 MHz – 1910 MHz	TDD
Band 36	1930 MHz – 1990 MHz	1930 MHz – 1990 MHz	TDD
Band 37	1910 MHz – 1930 MHz	1910 MHz – 1930 MHz	TDD
Band 38	2570 MHz – 2620 MHz	2570 MHz – 2620 MHz	TDD
Band 39	1880 MHz – 1920 MHz	1880 MHz – 1920 MHz	TDD
Band 40	2300 MHz – 2400 MHz	2300 MHz – 2400 MHz	TDD
Band 41	2496 MHz – 2690 MHz	2496 MHz – 2690 MHz	TDD
Band 42	3400 MHz – 3600 MHz	3400 MHz – 3600 MHz	TDD
Band 43	3600 MHz – 3800 MHz	3600 MHz – 3800 MHz	TDD
Band 44	703 MHz – 803 MHz	703 MHz – 803 MHz	TDD
Band 45	1447 MHz – 1467 MHz	1447 MHz – 1467 MHz	TDD
Band 46	5150 MHz – 5925 MHz	5150 MHz – 5925 MHz	TDD
Band 47	5855 MHz – 5925 MHz	5855 MHz – 5925 MHz	TDD
Band 65	1920 MHz – 2010 MHz	2110 MHz – 2200 MHz	FDD
Band 66	1710 MHz – 1780 MHz	2110 MHz – 2200 MHz	FDD
Band 67	DL only	738 MHz – 758 MHz	FDD
Band 68	698 MHz – 728 MHz	753 MHz – 783 MHz	FDD
Band 69	DL only	2570 MHz – 2620 MHz	FDD

Band 70	1695 MHz – 1710 MHz	1995 MHz – 2020 MHz	FDD
Band 71	663 MHz – 698 MHz	617 MHz – 652 MHz	FDD
Band 252	DL only	5150 MHz – 5250 MHz	FDD
Band 253	DL only	5725 MHz – 5850 MHz	FDD

Appendix 2 NR FR1 frequency bands [49]

NR Frequency bands	Uplink channel	Downlink channel	Duplex Mode
n1	1920 MHz – 1980 MHz	2110 MHz – 2170 MHz	FDD
n2	1850 MHz – 1910 MHz	1930 MHz – 1990 MHz	FDD
n3	1710 MHz – 1785 MHz	1805 MHz – 1880 MHz	FDD
n5	824 MHz – 849 MHz	869 MHz – 894 MHz	FDD
n7	2500 MHz – 2570 MHz	2620 MHz – 2690 MHz	FDD
n8	880 MHz – 915 MHz	925 MHz – 960 MHz	FDD
n12	699 MHz – 716 MHz	729 MHz – 746 MHz	FDD
n14	788 MHz – 798 MHz	758 MHz – 768 MHz	FDD
n18	815 MHz – 830 MHz	860 MHz – 875 MHz	FDD
n20	832 MHz – 862 MHz	791 MHz – 821 MHz	FDD
n25	1850 MHz – 1915 MHz	1930 MHz – 1995 MHz	FDD
n28	703 MHz – 748 MHz	758 MHz – 803 MHz	FDD
n30	2305 MHz – 2315 MHz	2350 MHz – 2360 MHz	FDD
n34	2010 MHz – 2025 MHz	2010 MHz – 2025 MHz	TDD
n38	2570 MHz – 2620 MHz	2570 MHz – 2620 MHz	TDD
n39	1880 MHz – 1920 MHz	1880 MHz – 1920 MHz	TDD
n40	2300 MHz – 2400 MHz	2300 MHz – 2400 MHz	TDD
n41	2496 MHz – 2690 MHz	2496 MHz – 2690 MHz	TDD
n48	3550 MHz – 3700 MHz	3550 MHz – 3700 MHz	TDD
n50	1432 MHz – 1517 MHz	1432 MHz – 1517 MHz	TDD
n51	1427 MHz – 1432 MHz	1427 MHz – 1432 MHz	TDD
n65	1920 MHz – 2010 MHz	2110 MHz – 2200 MHz	FDD
n66	1710 MHz – 1780 MHz	2110 MHz – 2200 MHz	FDD

n70	1695 MHz – 1710 MHz	1995 MHz – 2020 MHz	FDD
n71	663 MHz – 698 MHz	617 MHz – 652 MHz	FDD
n74	1427 MHz – 1470 MHz	1475 MHz – 1518 MHz	FDD
n75	DL only	1432 MHz – 1517 MHz	FDD
n76	DL only	1427 MHz – 1432 MHz	FDD
n77	3300 MHz – 4200 MHz	3300 MHz – 4200 MHz	TDD
n78	3300 MHz – 3800 MHz	3300 MHz – 3800 MHz	TDD
n79	4400 MHz – 5000 MHz	4400 MHz – 5000 MHz	TDD
n80	1710 MHz – 1785 MHz	UL only	FDD
n81	880 MHz – 915 MHz	UL only	FDD
n82	832 MHz – 862 MHz	UL only	FDD
n83	703 MHz – 748 MHz	UL only	FDD
n84	1920 MHz – 1980 MHz	UL only	FDD
n86	1710 MHz – 1780 MHz	UL only	FDD
n90	2496 MHz – 2690 MHz	2496 MHz – 2690 MHz	TDD

Appendix 3 NR FR2 frequency bands [50]

NR Frequency bands	Uplink Channel	Downlink Channel	Duplex Mode
n257	26500 MHz – 29500 MHz	26500 MHz – 29500 MHz	TDD
n258	24250 MHz – 27500 MHz	24250 MHz – 27500 MHz	TDD
n260	37000 MHz – 40000 MHz	37000 MHz – 40000 MHz	TDD
n261	27500 MHz – 28350 MHz	27500 MHz – 28350 MHz	TDD